**TITLE:** Environmental and Biological Drivers of Otolith Trace Element Composition in Staghorn Sculpin (*Leptocottus armatus*)

**AUTHORS:** Craig R. Norrie*[1,2], Thomas P. Hurst[3], Jessica A. Miller[4]

*Corresponding author: cnorrie@uw.edu

[1]Cooperative Institute for Marine Ecosystem and Resources Studies, Oregon State University, Newport, OR 97365, USA. ORCID: 0000-0003-0085-7314

[2]Current Address: School of Aquatic and Fishery Sciences. University of Washington Seattle, Washington, USA.

[3]Fisheries Behavioral Ecology Program, Resource Assessment and Conservation Engineering Division, Alaska Fisheries Science Center, National Marine Fisheries Service, National Oceanic and Atmospheric Administration, Hatfield Marine Science Center, Newport, OR, United States. ORCID: 0000-0002-1446-1540

[4]Department of Fisheries, Wildlife, and Conservation Sciences, Coastal Oregon Marine Experiment Station, Oregon State University, Newport, OR 97365, USA. ORCID: 0000-0002-6491-4085

**ABSTRACT:** Using of calcium carbonate ($CaCO_3$) structures as an ecological tool relies on the assumption that, for some elements, their composition is influenced by the water in which an organism lives. However biological processes including, growth rates, diet, ontogeny, reproductive state, or genetics can also influence their composition. It is essential we understand how intrinsic biological factors, external environmental conditions, and interactions impact the composition of $CaCO_3$ structures to make ecological inferences. We examined how temperature, pH, growth, and body size influenced elemental composition of staghorn sculpin (*Leptocottus armatus*) otoliths. We held animals (108-183 mm length) under three pH (7.60, 7.75, and 7.96) and two temperature (11.5 °C and 14.0 °C) treatments and examined relationships of three trace element:calcium ratios (Sr:Ca, Ba:Ca, B:Ca) to experimental conditions and body size. Sr:Ca ratios showed a temperature × size interaction, with smaller fish at 11.5 °C having higher values than those at 14.0 °C, while differences between temperatures diminished at larger sizes. Ba:Ca ratios were lower at 14.0 °C across sizes, indicating consistent temperature effects. B:Ca ratios showed weak but statistically significant negative relationships with size. No consistent effects of pH or growth rate were observed. Results highlight that trace element:calcium ratios vary in sensitivity to intrinsic and extrinsic factors, with Sr:Ca influenced by both temperature and body size, Ba:Ca reflecting moderate environmental effects, and B:Ca responding primarily to biological variation. Findings reinforce the value of otolith chemistry as an ecological tool, while emphasising the importance of considering individual-level variation when interpreting elemental signatures.

**KEYWORDS**: Otolith Chemistry, Calcium Carbonate, LA-ICP-MS, Growth, Size, Strontium

## INTRODUCTION

Elemental analysis of calcium carbonate ($CaCO_3$) structures such as otoliths, shells, and coral skeletons is used widely to address ecological questions. These structures have been used in several contexts including understanding larval dispersal patterns (Norrie et al. 2020), reconstructing migration trajectories (Miller et al. 2010), stock discrimination (Tanner et al. 2016), age estimate corroborations (e.g. Hüssy et al 2015), and climate reconstructions (Amekawa et al. 2016). While the application of these methods generally relies on the assumption that, for certain elements, the composition of $CaCO_3$ structures reflects the physiochemical properties of the water in which an animal resides, biological conditions such as growth rates, diet, ontogeny, reproductive state, and genetic differences can also influence their elemental composition (Sturrock et al. 2015, Izzo et al. 2018, Norrie et al. 2019, Miller & Hurst 2020). To make ecologically useful inferences it is essential to understand how intrinsic biological factors, external environmental conditions, and their interactions impact trace elemental composition.

There is particular interest in using the trace elemental composition of $CaCO_3$ structures to reconstruct organismal exposure to stressors associated with climate change such as increased temperatures, decreased pH, or reduced dissolved oxygen (Limburg et al. 2015, Tanaka et al. 2015, Reis-Santos et al. 2023). For these reconstructions to provide useful information, however, it is essential that there is a predictable relationship between trace element levels within the $CaCO_3$ matrix and the environmental variable of interest. The elemental composition of calcium carbonate structures is influenced by a range of environmental factors, including the concentration of dissolved elements, temperature, pH, and salinity (e.g. Miller 2009, Tian et al. 2021, Wu et al. 2025). Importantly, the degree to which environmental signals are expressed varies between internally and externally calcifying organisms. In organisms that precipitate $CaCO_3$ in direct contact with seawater such as bivalves and corals, in addition to the concentration of elements in the surrounding seawater, the elemental composition of carbonate structures can reflect environmental variables such as pH (Levin & Frieder 2015, Norrie et al. 2018), temperature (Wanamaker et al. 2008, D'Olivo et al. 2018), and estuarine dynamics such as freshwater inputs or diatom blooms (Gillikin et al. 2006, Thébault et al. 2009). In contrast to external calcifiers, otoliths which are the primary focus of $CaCO_3$ studies in most fish, form

internally. Otoliths are calcium carbonate structures located in the inner ear of teleost fish that are used for hearing and balance. Because they are not precipitated in direct contact with seawater, trace elements must be absorbed across the gills or gut and transported through the bloodstream to the endolymph before reaching the site of otolith biomineralisation (Sturrock et al. 2015; Loewen et al. 2016; Thomas et al. 2017). During this transport process, elements pass through several epithelial and physiological barriers, making their incorporation subject to physiological influences in addition to environmental ones.

Physiological effects may explain some of the different relationships between environmental variables and otolith composition that have been observed across studies. For example, the influence of temperature on otolith chemistry is widely reported, but its magnitude and direction can vary by species and context (e.g. Table 2 in Miller and Hurst 2020). Understanding elemental incorporation under realistic climate change scenarios is critical. Consequently, there is particular interest in using the trace elemental composition of CaCO3 structures to reconstruct organismal exposure to climate change stressors such as increased temperatures and decreased pH (ocean acidification) (Limburg et al. 2015, Tanaka et al. 2015, Reis-Santos et al. 2023). While pH effects have been observed in external calcifiers (Levin and Frieder 2015; Norrie et al. 2018; Gagnon et al. 2021), likely due to changes in relative availability of the borate ion $B(OH)_4^-$ at different pH levels, they have not been consistently observed to impact otolith chemistry (Hurst et al. 2012; Martino et al. 2017). Despite this inconsistency, boron remains of significant interest because it is potentially a powerful proxy for pH and is one of the few potential elemental proxies available for ocean acidification exposure in biogenic calcium carbonate structures (e.g. Levin et al. 2015, Gagnon et al 2021).

For accurate interpretation of field studies, it is essential to understand how size and growth impact trace element chemistry. Trace elemental studies often involve collecting individuals from multiple locations (e.g. estuaries, bays, or coastal sites) under the assumption that the chemistry of recently deposited otolith material reflects the environmental conditions at the site of capture and that the individual has been at this location long enough for $CaCO_3$ material to accrete. This information can be used as a proxy for environmental conditions (Izzo et al. 2017, Limburg & Casini 2018) and the elemental composition of the otolith core can be used to assign individuals to their natal origin (Williams et al. 2018, Rogers et al. 2019).

However, if intrinsic factors such as size or growth rate significantly influence otolith composition as has previously been observed (e.g. Hüssy et al. 2024; Miller and Hurst 2020), these assumptions may not hold. By understanding how biological processes impact otolith microchemistry of individuals held under identical conditions, we can develop analytical and interpretative approaches that can account for such variation, thus improving the accuracy of ecological inferences. Specifically, distinguishing between the effects of size (as a covariate for scaling physiological processes and life stage) and growth rate (a dynamic, metabolic factor) is essential, as these variables may operate through different physiological pathways to influence element incorporation (Stanley et al. 2015; Grammer et al. 2017; Miller & Hurst 2020; Hüssy et al. 2021).

This study examined the incorporation of trace elements into otoliths of a common estuarine and marine fish, staghorn sculpin (*Leptocottus armatus*), under a combination of three pH conditions (ambient ~ 8.00, medium - 7.75, low - 7.60) and two temperature (11.5 °C and 14.0 °C) conditions. We assessed how interactions between these environmental conditions and individual size and growth impacted otolith trace elemental concentrations. Using an experimental design that simulated field studies where multiple individuals are sampled from locations under the assumption that all experience the same environmental conditions, we addressed the following questions: 1) Does the otolith trace elemental composition vary between individuals held under differing pH and temperature conditions? 2) Is otolith elemental composition related to body size or growth? 3) Is the otolith elemental composition affected by an interaction between environmental conditions and body morphometrics?

## METHODS

### Animal Husbandry

Adult staghorn sculpin (*Leptocottus armatus*) were captured from Yaquina Bay in Newport, Oregon, USA (44.618350, -124.057282) with a beach seine net in late October 2020 ($n$ = 71. Upon capture, fish were transported to Oregon State University's Hatfield Marine Science Center's Coastal Ecology Lab in Newport, Oregon. In the lab, adult fish were split equally between six 150 L treatment tanks with varying combinations of environmental conditions. Each experimental tank was randomly assigned to one of six treatments, which were combinations of three pH conditions (ambient ~ 8.00, medium - 7.75, low - 7.60) and two temperature conditions

(11.5 °C & 14.0 °C). The pH treatments spanned a range of 0.4 units, with the lowest pH chosen to reflect conditions experienced during upwelling events on the west coast of the USA, which can reach pH 7.6 or lower (Feely et al. 2018). The two temperature conditions represented a moderate +2.5° C temperature differential, which is consistent with natural environmental gradients experienced by staghorn sculpin across its broad distribution along the Pacific Coast of North America and aligns with a range of predicted thermal stress. These treatment levels were chosen based on ranges commonly investigated in studies assessing future ocean conditions (Gattuso et al. 2015; Jewett & Romanou 2017; Wuebbles et al. 2017).

We developed a pH conditioning system using a Honeywell Durafet pH monitoring and conditioning system based on Hurst et al. (2012, 2019). Briefly, coastal oceanic water was pumped from nearby Yaquina Bay during flooding tides into a 3 million litre water reservoir. Water was pumped from the reservoir through a sand filter to three pH conditioning tanks within the fish holding facility. Honeywell Durafet III probes in each conditioning tank continuously monitored pH and regulated the injection of carbon dioxide ($CO_2$) to maintain treatment pH levels (± 0.07). Water from conditioning tanks gravity fed into the six experimental treatment tanks where fish were held. Temperature was manipulated within experimental tanks using individual aquarium heaters coupled to individual thermostats. We recorded experimental parameters (temperature, pH, dissolved oxygen) daily, using handheld probes (YSI ProQuatro Multiparameter Meter, Xylen Inc, Washington DC, USA). As the experiment was conducted indoors a timer was used to match local light/dark cycles. See below for analyses of seawater elemental and carbonate system conditions.

We acclimated fish to laboratory conditions for two weeks at ambient conditions (~ 10°C, pH ~ 7.95) prior to starting the experiment. After this period, we adjusted the water temperature by 0.5 °C/day and pH by 0.1 unit/day until target conditions were achieved. Staghorn sculpin were then reared under experimental treatment conditions for three months (90 days). Fish were fed a combination of Mazuri® Omnivore Aquatic Gel Diet and minced herring. Biomass in each tank was calculated at the start of the experiment, and each tank was fed ad libitum, with any uneaten food removed daily. At the start, midpoint, and conclusion of the experiment, fish were weighed (to the nearest gram) and measured (total length – TL, to the nearest mm). Initial fish sizes were 89–159 mm total length (TL; 118.29 ± 2.2 mm SEM) and 9–50 g wet mass (24.4 ±

1.2 g SEM). Although fish were not individually marked, the size variation within each tank permitted unambiguous identification of individuals throughout the experiment, with identities used in the estimation of individual growth rates (Hurst et al. 2012, Miller & Hurst 2020).

At the end of the experiment, fish were sacrificed by immersion in 250 ml/L of tricaine methanesulfonate (MS-222) buffered to a pH of 8.0 with sodium bicarbonate (Institutional Animal Care and Use Committee permit number - 2020-0129). To account for the potential impacts of reproductive condition on otolith composition (e.g. Sturrock et al 2015), during dissection, gonads were visually inspected; and 20 individuals had discernible gonads. Otoliths were removed, cleaned by removing all adhering tissue and rinsing in Milli Q water, and stored dry prior to analyses. Otoliths were embedded in two-part epoxy resin and transverse sections were cut using a Buehler® IsoMet Low Speed cutting machine. Sectioned otoliths were mounted on a glass slide using thermoplastic resin and polished using 3M tri-mite wet-or-dry paper (240-2,000 grit) and diamond lapping film (1-30 µm).

**LA-ICP-MS analysis**

We analysed the trace elemental composition of one randomly selected otolith from each fish using laser ablation inductively coupled plasma mass spectrometry (LA-ICP-MS). We collected information on the concentrations of boron ($^{11}B$), strontium ($^{86}Sr$), barium ($^{137}Ba$). We selected strontium and barium as they are strongly linked to ambient water chemistry and are among the most widely used elements in otolith studies of salinity, temperature, and diadromy (Walther & Thorrold 2006; Hüssy et al 2020; Norrie et al. 2022; Reis-Santos et al. 2023). Boron was included because it has shown potential as a proxy for exposure to ocean acidification in biogenic calcium carbonate structures (Levin & Frieder 2015; Norrie et al. 2018; Limburg et al. 2023). As Co, Mn, and Mg were detectable in otolith alongside the focal elements they were also quantified. We used a Photon Machines Analyte G2 laser coupled to a Thermo Scientific X-Series II quadruple ICP-MS. We collected data along a 100-µm transect parallel to the otolith dorsal edge. We used counts of daily otolith increments to ensure that sampled otolith material was deposited while animals were held under experimental conditions (Laetz et al. 2024; Table S1). The laser operated at 7 Hz with an output of 75% and target energy of 7 J $cm^2$ with a spot size of 40 µm that travelled at 2 µm $s^{-1}$ across the sample. Mean daily otolith increment width was 1.6 µm (± 0.5 SEM), thus the 40 µm spot ablated material deposited over a 25-day period.

To remove any surface contamination each otolith was pre-ablated along the same transect used for sample analyses. The pre-ablation scan ran with at 2 Hz with a spot size of 50 µm and a speed of 100 µm $s^{-1}$. National Institute of Standards and Technology (NIST) 610 and 612 standards were analysed at the start and end of each day and after every 10 otoliths throughout for standardisation purposes and estimates of precision. USGS calcium carbonate standards MACS-1 and MACS-3 were also analysed at the start and end of each run for calculations of accuracy.

Otolith analyte count data were normalised by $^{43}Ca$ and trace element:calcium ratios (TE:Ca) are presented in µmol:mol (B:Ca, Ba:Ca) or mmol:mol (Sr:Ca). Data was converted to elemental ratios based on measurements of the NIST 612 standard. Precision (% RSD) was calculated from multiple analyses of NIST612 standard (B:Ca, 4.4 %, Sr:Ca = 1.5 %, Ba:Ca = 0.53 %). Accuracy was determined through repeated analysis of MACS-1 and MACS-3 standards (B:Ca = 98.9 %, Sr:Ca = 88.0%, Ba:Ca = 96.2 %). To describe elemental concentrations in each otolith TE:Ca values across each transect were averaged for each otolith.

**Water carbonate and trace element analysis**

To determine if there were any tank differences in trace element composition of water, we measured the Ca, Sr, Ba, and B levels in water samples collected from each experimental tank each month (total $n = 3$ from each tank) using a Spectros Arcos inductively coupled optical emissions spectrometer (ICP-OES) (Ca at 317.9 nm, B at 249.7 nm, Ba at 233.5 nm, and Sr at 460 nm). Prior to analysis, samples were filtered (0.25 µm) and acidified (< 2 pH) with ultrapure $HNO_3$. Matrix matched standards were created using SPEX Certiprep Group® certified reference materials and a NaCl solution. Accuracy was assessed based on repeated measurements ($n = 3$) of SLRS-6 river water certified reference material (B = 95.5%, Ba 97.8%, Ca = 98.1 %, Sr = 99.2%). Precision was estimated with repeated measurements of the same sample and varied by < 2% for each element. We compared the concentration of elements between experimental tanks using a one-way analysis of variance (ANOVA).

To parameterise the carbonate system, we collected 200 mL samples of seawater once a month which were preserved by the addition of 200 µL mercuric chloride ($HgCl_2$). Dissolved inorganic carbon (DIC) and total alkalinity (TA) were quantified at the Ocean Acidification Research Center at the University of Alaska at Fairbanks. An AIRICA (Automated InfraRed

Inorganic Carbon Analyzer) was used to measure DIC and a VINDTA 3C (Versatile Instrument for the Determination of Total dissolved inorganic carbon and Alkalinity) was used to measure TA. The AIRICA and VINDTA 3C instruments were calibrated using Certified Reference Materials (CRMs) from the Dickson Laboratory at the Scripps Institute of Oceanography and a daily correction was applied. Mean deviation of measurements from CRM values was $\pm 1.40$ μmol $kg^{-1}$ for DIC and $\pm 2.00$ μmol $kg^{-1}$ for TA. These measurements were used to calculate the pH and $CO_2$ conditions during the experiment based on the dissociation constants of Dickson and Millero (1987).

## Data analysis

### *Metrics of growth and condition*

We calculated mass specific (MSGR) and length specific (LSGR) growth rates (percentage increase per day) over the course of the experiment using the formula [ln(final size) - ln(initial size) / experimental duration (in days)]*100. We also used total change in the length-weight residuals (ΔLWR) over the course of this experiment to quantify changes in fish condition.

### *Impact of treatment conditions on body size, growth, and condition*

All statistical analyses were conducted in R (v 4.01 – R Core Team). We first examined if temperature and pH treatments impacted size (final mass and TL), growth (LSGR & MSGR), and condition (ΔLWR). We used linear models where temperature, pH, and their interaction were included as fixed effects. Where appropriate, response variables were log-transformed to meet model assumptions of homogeneity of variance and normality of residuals.

### *Relationships between individual size, growth, and otolith TE:Ca ratios*

We used linear models with categorical predictors (temperature, pH) and continuous predictors (body size, growth, and condition) to evaluate their effects and interactions on TE:Ca ratios (Sr:Ca, Ba:Ca, and B:Ca). To avoid issues of collinearity among biological traits, we ran separate models in which temperature, pH, and their interaction were assessed alongside a single biological predictor (length, mass, growth, or condition). Using an identical environmental structure across all models allowed direct comparison of the explanatory value of each biological

predictor. Because only the biological covariate varied between models, differences in model performance reflected the contribution of that predictor rather than differences in environmental model specification. TE:Ca ratios were log-transformed where necessary to meet assumptions of homogeneity of variance and normality of residuals. We then conducted post hoc pairwise tests using the emtrends function in the 'emmeans' package (Lenth et al. 2024).

This approach allowed us to evaluate whether individual-level biological variation contributed to differences in TE:Ca ratios within shared environmental conditions. It also allowed us to test whether the effects of biological covariates were consistent across temperature and pH treatments. In field studies, where individual variation is often uncontrolled, such effects could be misattributed to environmental differences among sites. To further assess the contribution of interaction terms, we compared reduced models containing only additive effects with full models that included temperature × size interactions using likelihood ratio tests. These tests were applied to models where temperature × size interactions were identified in the initial analyses. We also generated partial residual plots for the top models to visualise the relationships between biological variables and TE:Ca ratios (Figures S1-S4).

## RESULTS

### Water properties

In each tank, mean temperatures were within 0.4 °C of target temperatures over the course of the experiment (Table 1). Mean pH in the ambient treatment tanks was 7.96 and the other treatments were within 0.02 pH units of our targets. The trace elemental composition of seawater did not vary among treatments (Table 1) as one-way ANOVAs showed no significant differences existed in water levels of B:Ca ($F_{5,18}$=0.643, $p$=0.67), Sr:Ca ($F_{5,18}$ = 0.652, $p$ = 0.664) or Ba:Ca ($F_{5,18}$ = 1.469, $p$ = 0.248) ratios among tanks/treatments.

### Size, growth, and condition

Of 71 animals in the experiment, there were 9 mortalities (Table 2) but there was no clear pattern across treatments or obvious cause of the mortalities. Temperature and pH differences among tanks did not impact fish size, growth, or condition across treatment tanks as indicated by the lack of significant temperature, pH, or interaction effects for TL, mass, LSGR, MSGR, final LWR or ΔLWR (all $F_{1,56}$ < 1.25, p > 0.250). Final TL ranged from 108 to 183 mm with a mean

of 137.2 mm (± 2.5 SEM) and mass ranged from 14 to 79 g with a mean of 34.7 g (± 2.1 SEM). No significant differences in final size or growth existed between individuals with discernible gonads and those without (final mass: $t_{(52)} = -0.85$, $p = 0.40$; final length: $t_{(52)} = -1.05$, $p = 0.297$; LSGR : $t_{(52)} = 0.04$, $p = 0.80$; MSGR: $t_{(52)} = 0.89$, $p = 0.38$) and there were no patterns in maturity across tanks.

Table 1. Mean water properties (± SEM) and trace elemental composition over the course of this experiment. Abbreviations and units used in column headers: Salinity – salinity (PSU), TA- total alkalinity (µmol $kg^{-1}$), DIC - Dissolved inorganic carbon (µmol $kg^{-1}$), $pCO_2$ - $pCO_2$ (µatm), Calcite saturation state - $\Omega_{Calcite}$, Aragonite saturation state- $\Omega_{Aragonite}$. Sr:Ca – Sr:Ca (mmol:mol), B:Ca – B:Ca (µmol:mol), Ba:Ca – Ba:Ca (µmol:mol)

| Treatment Temp | Measured Temp | Treatment pH | Measured pH | Salinity | TA | DIC | $pCO_2$ | $\Omega_{Calcite}$ | $\Omega_{Aragonite}$ | TE:Ca ratio | | |
|---|---|---|---|---|---|---|---|---|---|---|---|---|
| | | | | | | | | | | Sr:Ca | B:Ca | Ba:Ca |
| | 11.6 | Ambient | 7.97 | 29.53 | 2036 | 1910 | 437.4 | 2.39 | 1.51 | 10.22 | 47.67 | 0.1 |
| 11.5 | (± 0.15) | (~7.96) | (± 0.01) | (± 0.24) | (± 23) | (± 24) | (± 13.5) | (± 0.02) | (± 0.01) | (± 0.22) | (± 0.94) | (± 0.01) |
| | 11.25 | | 7.78 | 29.53 | 2036 | 1963 | 677.4 | 1.68 | 1.06 | 9.67 | 45.15 | 0.06 |
| 11.5 | (± 0.15) | 7.80 | (± 0.02) | (± 0.24) | (± 21) | (± 28) | (± 65.0) | (± 0.12) | (± 0.07) | (± 0.73) | (± 3.39) | (± 0.01) |
| | 11.4 | | 7.67 | 29.53 | 2040 | 1985 | 802.5 | 1.48 | 0.93 | 10.00 | 46.56 | 0.06 |
| 11.5 | (± 0.14) | 7.65 | (± 0.02) | (± 0.24) | (± 17) | (± 26) | (± 87.3) | (± 0.1) | (± 0.06) | (± 0.22) | (± 1.01) | (± 0.00) |
| | 13.85 | Ambient | 7.95 | 29.53 | 2039 | 1922 | 534.9 | 2.29 | 1.45 | 9.70 | 45.20 | 0.07 |
| 14 | (± 0.1) | (~7.96) | (± 0.04) | (± 0.24) | (± 19) | (± 17) | (± 63.1) | (± 0.21) | (± 0.13) | (± 0.34) | (± 1.58) | (± 0.01) |
| | 13.58 | | 7.80 | 29.53 | 2038 | 1960 | 710.4 | 1.77 | 1.12 | 10.12 | 47.24 | 0.08 |
| 14 | (± 0.07) | 7.80 | (± 0.04) | (± 0.24) | (± 18) | (± 26) | (± 67.3) | (± 0.1) | (± 0.06) | (± 0.24) | (± 1.12) | (± 0.01) |
| | 13.68 | | 7.66 | 29.53 | 2037 | 1971 | 805.8 | 1.63 | 1.03 | 10.68 | 49.76 | 0.08 |
| 14 | (± 0.23) | 7.65 | (± 0.01) | (± 0.24) | (± 19) | (± 35) | (± 114. 8) | (± 0.2) | (± 0.13) | (± 0.69) | (± 3.28) | (± 0.02) |

Table 2. Mean biological attributes (± SEM) of fish from each tank at the conclusion of this study. TL = total length (mm), LSGR = Length specific growth rate (% total length day$^{-1}$), Mass (grams), MSG = mass specific growth rate (% body weight day$^{-1}$), LWR = Length weight residuals, Δ LWR = change in length weight residuals, *n* (mort.) = sample size - mortalities that occurred throughout the experiment shown in brackets.

| Temp | pH | Initial TL | Final TL | LSGR | Initial Mass | Final Mass | MSGR | LWR | Δ LWR | n (mort.) |
|---|---|---|---|---|---|---|---|---|---|---|
| 11.5 | Ambient | 119 (± 3) | 142 (± 5) | 0.18 (± 0.02) | 23 (± 3) | 35 (± 4) | 3.65 (± 0.18) | -2.0 (± 2.5) | -4.3 (± 2.3) | 12 (0) |
| 11.5 | Medium | 123 (± 5) | 139 (± 5) | 0.15 (± 0.02) | 21 (± 2) | 37 (± 5) | 3.87 (± 0.18) | 2.7 (± 1.5) | 4.1 (± 2.4) | 10 (2) |
| 11.5 | Low | 115 (± 6) | 135 (± 6) | 0.20 (± 0.01) | 20 (± 3) | 33 (± 5) | 3.80 (± 0.12) | 0.8 (± 1.2) | -1.9 (± 2.4) | 10 (2) |
| 14 | Ambient | 119 (± 6) | 136 (± 7) | 0.17 (± 0.02) | 19 (± 3) | 34 (± 6) | 3.71 (± 0.16) | 1.8 (± 2.0) | 2.9 (± 2.7) | 10 (2) |
| 14 | Medium | 116 (± 7) | 137 (± 11) | 0.14 (± 0.03) | 23 (± 5) | 39 (± 10) | 3.61 (± 0.30) | 5.8 (± 2.2) | 2.3 (± 3.6) | 8 (3) |
| 14 | Low | 114 (± 5) | 133 (± 5) | 0.17 (± 0.01) | 19 (± 3) | 31 (± 4) | 3.60 (± 0.17) | 0.5 (± 1.6) | -1.3 (± 1.5) | 12 (0) |

282

## Otolith trace elemental composition

Overall, for B:Ca, Ba:Ca, and Sr:Ca, models that included body size metrics (length or mass) as covariates explained more variation in otolith trace element ratios than models including other biological covariates such as growth rate or condition as shown by the higher model $R^2$ values (Table 3; Table 4). These models typically explained between ~12–36% of the variation depending on the element examined. In some cases, body size also interacted with environmental variables. Otolith Co:Ca, Mn:Ca, and Mg:Ca showed low explanatory power ($R^2 < 0.1$) and no consistent treatment responses (Table S2).

### *Strontium*

Otolith strontium levels were influenced by an interaction between temperature and body size. Individuals from the 11.5 °C temperature treatment exhibited a significant negative relationship between size and Sr:Ca ratios, while at 14.0 °C this relationship was weaker (Figure 4; Table 3; Table 4). The slope between Sr:Ca and final length was −1.04 at 11.5 °C and −0.34 at 14.0 °C, while for final mass the slope was −0.35 at 11.5 °C and −0.10 at 14.0 °C. This indicated that Sr:Ca declined approximately three times more steeply with increasing size in colder water. This resulted in Sr:Ca ratios in smaller individuals being approximately 20% higher than larger fish the 11.5 °C treatment. There were no significant effects of pH, LSGR, MSGR, or ΔLWR on Sr:Ca ratios ($p > 0.2$). Likelihood ratio tests supported the inclusion of the temperature × size interaction in the Sr:Ca models. The interaction significantly improved model fit in both the mass model ($\chi^2_1 = 8.19$, $p = 0.004$) and the length model ($\chi^2_1 = 6.97$, $p = 0.008$).

Table 3. Mean otolith trace element:calcium (± SE) ratios of staghorn sculpin held under a combination of varying pH and temperature conditions.

| Temp | pH | Sr:Ca (mmol:mol) | B:Ca (µmol:mol) | Ba:Ca (µmol:mol) |
|---|---|---|---|---|
| 11.5 | Ambient | 1.96 (± 0.11) | 26.4 (± 5.75) | 1.34 (± 0.1) |
| 11.5 | Medium | 2.02 (± 0.13) | 25.43 (± 4.28) | 1.36 (± 0.18) |
| 11.5 | Low | 2.23 (± 0.15) | 33.95 (± 5.65) | 1.41 (± 0.12) |
| 14 | Ambient | 1.96 (± 0.12) | 22.26 (± 3.46) | 1.24 (± 0.14) |

| | | | | |
|---|---|---|---|---|
| 14 | Medium | 1.86 (± 0.11) | 33.2 (± 11.45) | 1.32 (± 0.13) |
| 14 | Low | 1.82 (± 0.04) | 19.43 (± 2.3) | 0.99 (± 0.04) |

303

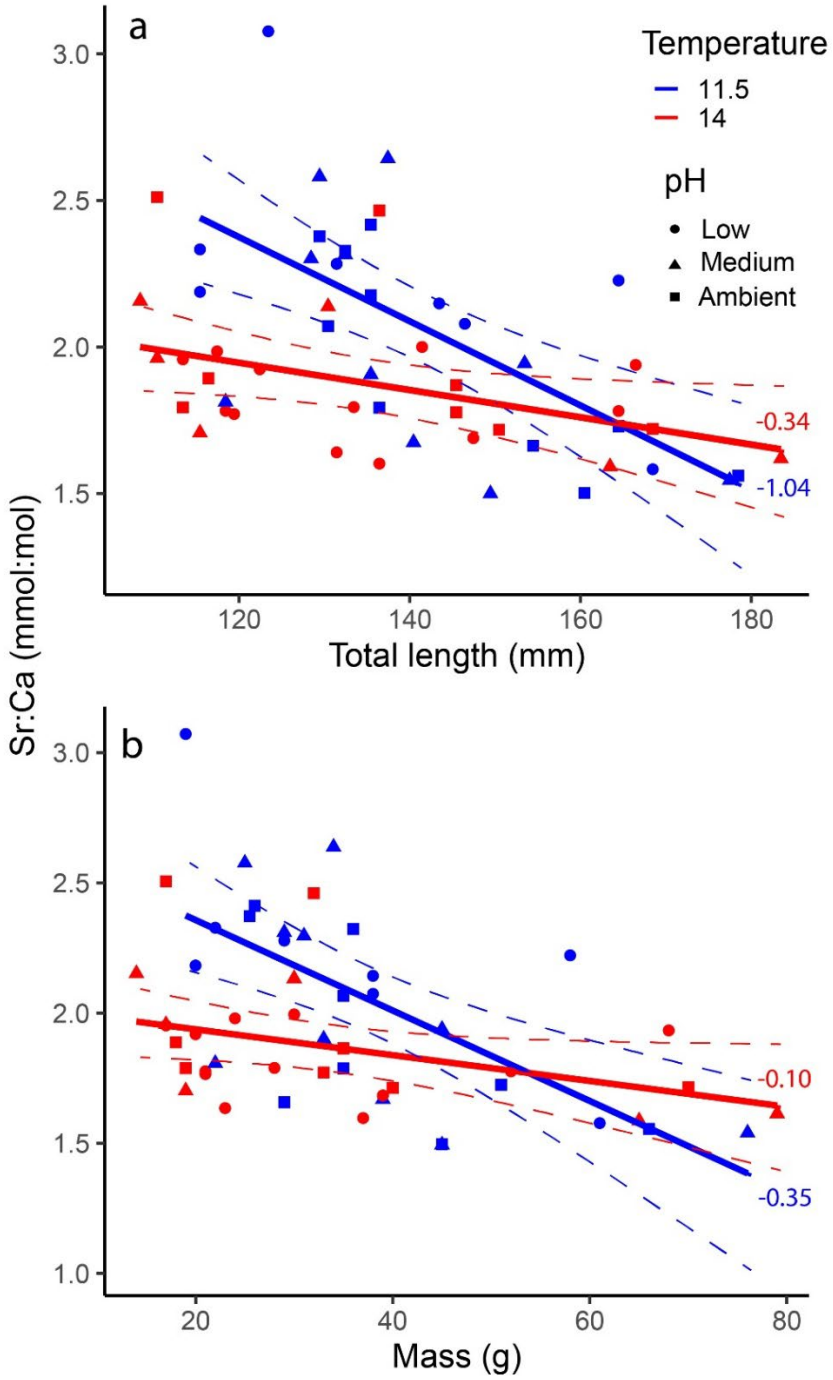


304

305 Figure 4. Relationship between individual A) total length and B) individual mass and Sr:Ca
306 ratios for individuals pooled across pH treatments. Dotted lines show 95 % confidence intervals

and numbers show slopes of the relationship between body size and Sr:Ca and size for each temperature treatment.

Table 4. *p* values, adjusted $R^2$, and AIC values from linear models examining covariates of final length, final mass, length specific and mass specific (MSGR) growth rates, and length weight residuals (LWR) for each trace element calcium ratio (TE:Ca) investigated in this work. Bold values indicate $p < 0.05$. For full results including F values and DF see supplementary Table S3.

| | | ***p* values** | | | | | | | | |
|---|---|---|---|---|---|---|---|---|---|---|
| **TE:Ca** | **Covariate** | **Temp x pH x covariate** | **pH x covariate** | **Temp x covariate** | **Temp x pH** | **Covariate** | **pH** | **Temp** | **Model adjusted $r^2$** | **AIC** |
| Sr:Ca | Final Length | 0.93 | 0.39 | **0.02** | 0.13 | **<0.001** | 0.69 | **0.02** | 0.3629 | -52.984 |
| | Final Mass | 0.84 | 0.59 | **0.02** | 0.08 | **<0.001** | 0.69 | **0.03** | 0.3305 | -48.642 |
| | LSGR | 0.72 | 0.49 | 0.56 | 0.28 | 0.21 | 0.79 | 0.07 | -0.0062 | -28.301 |
| | MSGR | 0.38 | 0.18 | 0.35 | 0.13 | 0.22 | 0.76 | 0.07 | 0.0952 | -32.675 |
| | LWR | 0.25 | 0.16 | 0.73 | 0.12 | 0.35 | 0.73 | 0.07 | 0.09297 | -34.384 |
| B:Ca | Final Length | 0.23 | 0.48 | 0.79 | 0.11 | **0.01** | 0.71 | 0.21 | 0.1273 | 85.439 |
| | Final Mass | 0.09 | 0.47 | 0.85 | **0.05** | **0.05** | 0.43 | 0.31 | 0.1491 | 76.932 |
| | LSGR | 0.99 | 0.85 | 0.6 | 0.24 | 0.12 | 0.75 | 0.26 | -0.05889 | 95.88 |
| | MSGR | 0.67 | 0.11 | 0.33 | 0.1 | 0.13 | 0.45 | 0.33 | 0.09354 | 82.306 |
| | LWR | 0.92 | 0.06 | 0.68 | 0.13 | 0.65 | 0.59 | **0.04** | 0.06913 | 84.187 |
| Ba:Ca | Final Length | **0.03** | 0.13 | 0.49 | 0.1 | **0.02** | 0.44 | **0.01** | 0.284 | 11.049 |
| | Final Mass | 0.08 | 0.17 | 0.56 | 0.08 | **0.03** | 0.5 | **0.02** | 0.2341 | 17.934 |
| | LSGR | 0.45 | 0.56 | 0.77 | 0.2 | 0.4 | 0.54 | **0.03** | 0.0409 | 26.859 |
| | MSGR | 0.95 | 0.33 | 0.51 | 0.2 | 0.22 | 0.57 | **0.04** | 0.04313 | 25.7 |
| | LWR | 0.06 | 0.78 | 0.92 | 0.07 | 0.81 | 0.46 | 0.31 | 0.09491 | 21.967 |

309

***Boron***

Body size weakly, but significantly impacted B:Ca ratios, with negative relationships observed for both total length and mass (Table 4; Figure 5). Boron levels were not affected by interactions between biological and environmental variables. The slope of the relationship between mass and B:Ca ratios was -0.04, whereas the relationship between total length and B:Ca was -0.02. LSGR, MSGR, and ΔLWR were not significantly related to B:Ca ratios (Table 4).

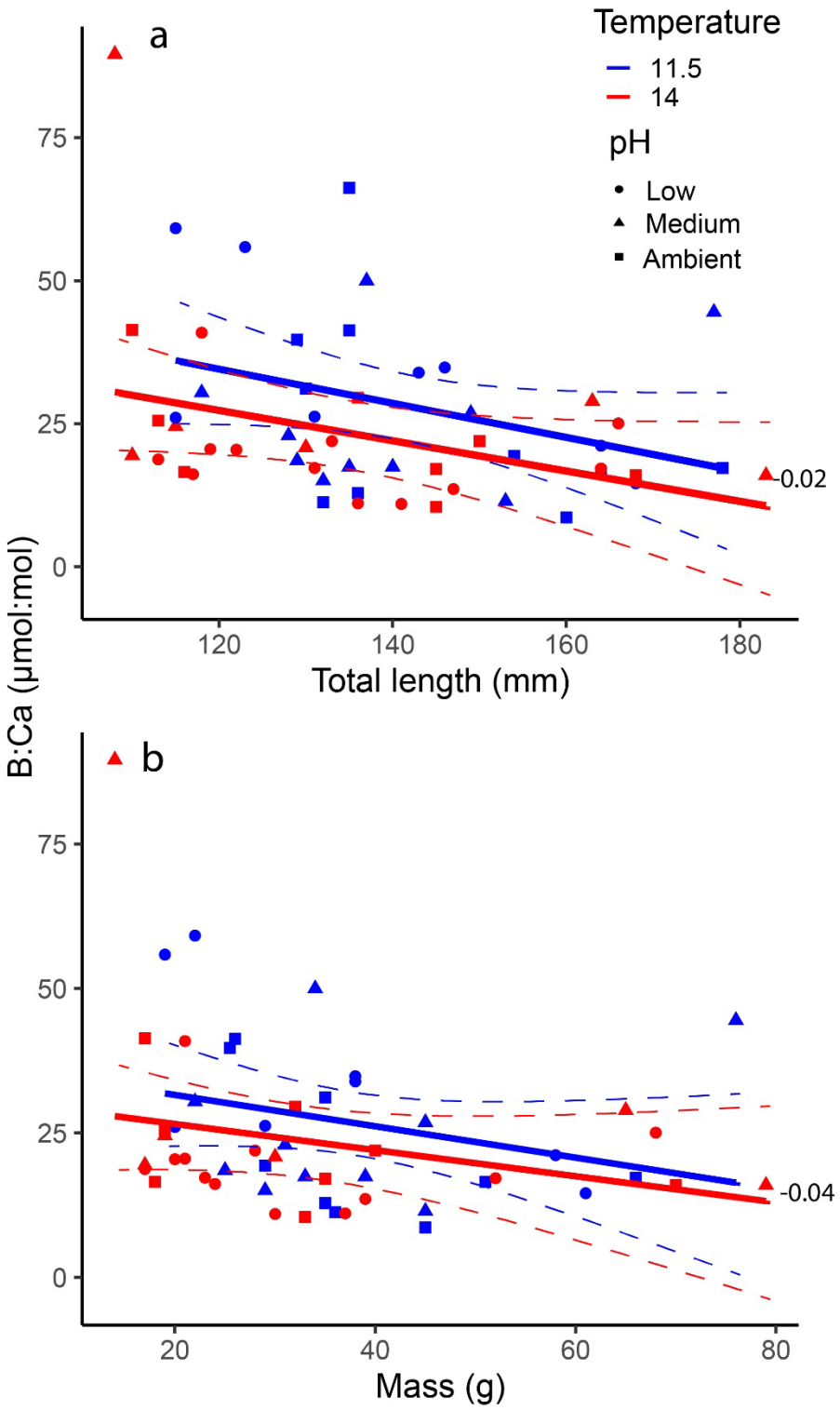


316

317 Figure 5. Relationship between individual A) total length and B) individual mass and B:Ca
318 ratios. Dotted lines show 95 % confidence intervals and numbers show the slope of the
319 relationship between body size and B:Ca ratios.

***Barium***

There was a consistent negative effect of temperature on Ba:Ca ratios with significant temperature effects in all but one of the models (Table 4; Figure 6). In the model that included total length as a covariate we observed a significant total length*pH*temperature interaction effect (Table 4). Likelihood ratio tests did not support a temperature × size interaction for Ba:Ca. Adding the interaction did not improve model fit in either the mass model ($\chi^2_1 = 0.45$, $p = 0.50$) or the length model ($\chi^2_1 = 0.42$, $p = 0.52$). There was a weak, but significant, negative effect of mass on Ba:Ca (slope = -0.004). No impacts of growth or condition on Ba:Ca was observed.

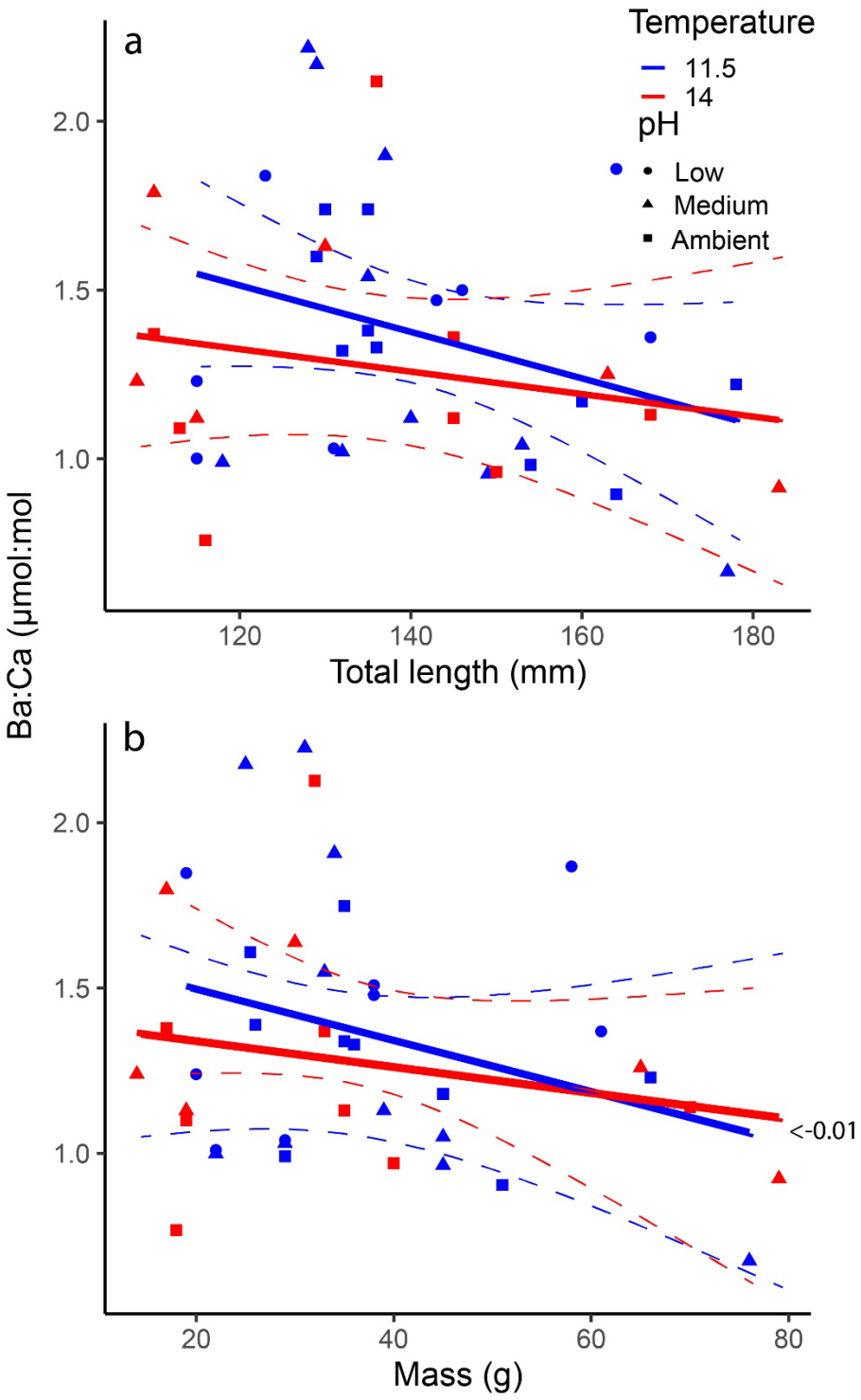


328

329 Figure 6. Relationship between a) total length b) mass and Ba:Ca ratios in otolith of staghorn
330 sculpin held at 11.5 °C and 14 °C. Dotted lines show 95 % confidence intervals. Numbers show
331 the slope of the relationship between body size and Ba:Ca ratios where a significant main effect
332 existed.

## DISCUSSION

Spatial variation in the concentration of certain trace elements in otoliths is often interpreted as being due to environmental differences between locations. Based on this interpretation otolith chemistry can serve as a useful marker in studies of distribution, movement, mixing, and, possibly, serve as a proxy for environmental conditions. The potential for biological processes to confound these interpretations has become clearer over recent decades (e.g. Sturrock et al. 2015, Stanley et al. 2015, Miller & Hurst 2020). Few studies, however, explicitly determine how individual size influences otolith chemistry or if size interacts with environmental conditions in determining elemental composition under controlled experimental conditions. Here we used an approach that mimicked field studies that examine individuals from distinct geographic locations (e.g. Grammer et al. 2017, Pease et al. 2023) and demonstrated that biological (i.e. size) and environmental variables (i.e. pH/temperature) can impact trace element levels, both independently and interactively. As each environmental treatment was represented by a single tank, tank-specific influences cannot be fully separated from temperature and pH treatments, so environmental effects should be interpreted with appropriate caution. Of the elements we analysed, strontium, barium, and boron were influenced by biological and/or environmental factors. Our results emphasise previous work showing that physiological attributes such as size and growth should be accounted for when making ecological inferences using otolith trace elements to avoid confounding environmental interpretations (Sturrock et al. 2015, Grammer et al. 2017, Izzo et al. 2018).

### Strontium

Strontium is one of the most frequently used elements in otolith trace elemental studies as it reflects environmental conditions (Doubleday et al. 2014, Reis-Santos et al 2018, Norrie et al 2022). Otolith strontium levels track ambient concentrations (Elsdon & Gillanders 2003, Walther & Thorrold 2006) because $Sr^{2+}$ has a similar ionic radius to $Ca^{2+}$ and can easily substitute for calcium in the $CaCO_3$ lattice (Doubleday et al 2014; Thomas et al. 2017). Thus, Sr:Ca ratios are commonly used to reconstruct salinity due to the higher levels of strontium in seawater than in most freshwater systems, and can also complement isotopic methods for reconstructing freshwater migration trajectories (Kraus & Secor 2004, Tian et al. 2021; Avigliano et al. 2021). Sr:Ca ratios have also been shown to vary with temperature, although the direction and

363 magnitude of this relationship is inconsistent (Sturrock et al. 2015, Miller and Hurst 2020), and it
364 is often included in multi-elemental suites used for stock delineation and dispersal studies (e.g.
365 Tanner et al 2016, Rogers et al. 2019, Teichert et al. 2024). Our results, which show an
366 interactive effect of body size and temperature on otolith strontium levels, add to the growing
367 body of evidence that, in addition to environmental influences, organismal physiology can
368 impact otolith strontium levels (Sturrock et al. 2015, Grammer et al. 2017, Hüssy et al. 2021) and
369 highlight the need to explicitly account for these effects in field studies.

370 To understand how our results could impact the interpretation of field studies, it is
371 important to compare the scale of variation we observed with those documented in situ. Previous
372 work on this same species (Miller 2007) reported mean Sr:Ca differences of ~10% between
373 estuaries located 200–400 km apart along the Oregon coast. Similarly, studies of other species
374 have detected mean differences in Sr:Ca ratios of 10–20% between sites separated by less than
375 50 km (e.g. Barnes and Gillanders 2013; Mohan and Walther 2015; Williams et al. 2018). Based
376 on our model predictions, the smallest individual from the 11.5 °C treatment in our study (111
377 mm TL) would have a Sr:Ca ratio 35% higher than that of the largest individual (178 mm TL)
378 from the same treatment. This inter-individual effect is larger than the mean inter-site differences
379 reported at smaller spatial scales, but smaller than the maximum inter-estuary difference of 114%
380 reported in Miller (2007). At these smaller scales environmental gradients are likely to be
381 narrower which suggests that differences in size or physiology may contribute more substantially
382 to otolith variation than spatial environmental differences. In such cases, differences in Sr:Ca
383 may be misinterpreted as environmental in origin (e.g., salinity differences between habitats)
384 when they may instead reflect biological effects. Indeed, these biological effects may explain
385 some of the variation in strontium levels observed over relatively small scales where
386 environmental conditions may be consistent (Mateo et al. 2012; Aschenbrenner et al. 2016;
387 Williams et al. 2018). Maturity can alter energy allocation and ion regulation, which in turn
388 could affect element incorporation into calcified structures (Sturrock et al. 2015). However, no
389 differences in size or growth were detected between fish with and without gonads, and maturity
390 showed no consistent patterns across tanks, suggesting that reproductive state was not likely the
391 driver of the size-related Sr:Ca patterns observed here. Together, these results reinforce that body
392 size rather than maturity status is the key biological factor underlying Sr variation in our study.

When using trace elements to assign individuals to a collection or natal location, strontium is generally used as part of a multi-elemental suite. The relative contribution of strontium to the site classification can vary. Thus, carefully balancing the site level discrimination provided by including strontium with potential risks associated with inter individual variation should be carefully considered when using this trace element. This could be achieved by restricting comparisons to individuals of similar life stages or by explicitly including a size covariate in classification models. While size-related variation in Sr:Ca may affect fine-scale spatial assignments, it is unlikely to influence migratory reconstructions in anadromous fish, which rely on detecting large intra-individual shifts between freshwater and marine environments of up to 400% as the concentration as environmental strontium changes between freshwater and marine habitats (Izzo et al. 2018; Austin et al. 2019; Norrie et al. 2022).

Understanding the mechanisms underlying the interactive effects of size and temperature on strontium incorporation into otoliths is challenging. However, size-related physiological differences likely influence how strontium is processed and partitioned during otolith formation. Elements present as free ions in the endolymph are more likely to substitute for $Ca^{2+}$ in the $CaCO_3$ fraction and thus reflect ambient strontium concentrations, while those bound to proteins are more likely to be incorporated into the organic matrix and influenced by physiological processes. Because strontium occurs in both fractions (Thomas et al. 2017), this dual incorporation pathway complicates the interpretation of strontium signals in otoliths. While previous work has shown negative relationships between growth and Sr:Ca ratios (Stanley et al. 2015; Miller & Hurst 2020) we did not observe any impact of growth rates on strontium levels in our work. This suggests that size-related variation in Sr:Ca may arise independently of growth rate, highlighting the importance of considering physiological traits beyond growth alone such as metabolism when interpreting otolith chemistry.

**Barium**

Although water barium concentrations are the dominant driver of otolith Ba:Ca ratios (Elsdon & Gillanders 2003, Walther & Thorrold 2006, Reis-Santos et al. 2013), negative relationships have also been found between barium levels and growth rates (Miller 2011, Sturrock et al. 2015), salinity (Reis-Santos et al. 2013, Barnes and Gillanders 2013, Stanley et al. 2015), and temperature (Elsdon and Gillanders 2002, 2004; Miller 2009; Barnes and Gillanders

2013; Reis-Santos et al. 2013; Stanley et al. 2015). Ba:Ca can also be impacted by diet (Webb et al. 2012, Izzo et al. 2015). The three-way interaction between body size, pH, and temperature, together with the main effects of temperature and body size, highlight the impact of environmental and biological factors on otolith Ba:Ca ratios.

Along with strontium, barium is often frequently included in multi-elemental suites used to reconstruct dispersal pathways (e.g. Matta et al. 2019, Beer et al 2011) and has been used to reconstruct salinity histories of individuals (e.g. Elsdon & Gillanders 2005, Miller 2011, Shima & Swearer 2016). Although there was a significant negative effect of body size on Ba:Ca ratios, this effect was relatively weak, so it is unlikely to obscure spatial differences in otolith chemistry. For example, the largest pairwise difference in mean Ba:Ca ratios between tanks in our study was approximately 140% (0.99 μmol:mol vs 1.41 μmol:mol), whereas differences of 150 – 200% have been reported to exist between different sites within estuaries or between closely located (10s of km) estuaries (Miller 2007, Barnes and Gillanders 2013). This suggests that, over broad spatial scales, the size-related variation observed in our study is unlikely to compromise the utility of Ba:Ca for ecological classification.

Like strontium, barium can substitute for $Ca^{2+}$ in the $CaCO_3$ matrix and be incorporated into the proteinaceous fraction of the otolith (Thomas et al. 2017). This dual incorporation pathway suggests that both environmental and physiological processes may influence Ba:Ca ratios. For example, free $Ba^{2+}$ ions are more likely to be incorporated into the carbonate matrix and thus reflect ambient concentrations, while protein-bound barium may be more sensitive to individual physiology. Processes such as ion transport, protein synthesis, and metabolic activity could therefore contribute to residual variation in Ba:Ca ratios even under stable environmental conditions (Loewen et al. 2016; Sturrock et al. 2015, Hüssy et al. 2021). While the effects observed here were small, considering individual characteristics such as body size may improve the interpretation of otolith Ba:Ca patterns in ecological studies.

**Boron**

Although recent studies suggest links between boron incorporation into carbonate structures and dissolved oxygen and pH variability (Norrie et al. 2018; Cavole et al. 2023; Limburg et al. 2023), the environmental drivers of B:Ca ratios in fish otoliths remain poorly defined. In our study, body size had a weak but statistically significant effect on B:Ca ratios,

while no consistent effects of pH were observed. B:Ca only varied with temperature in one model, and this was dependent on the inclusion of a condition index as a covariate. Our results are consistent with Matta et al. (2019), who also reported a negative relationship between body size and B:Ca ratios in juvenile fish. However, the magnitude of biologically driven variation in our study was small: for example, the predicted ~50% difference in B:Ca between the smallest and largest individuals was less than the 70–300% variation reported across spatial or environmental gradients in field studies (e.g., Limburg et al. 2023; Matta et al. 2019; Cavole et al. 2023). This suggests that, in most field applications, size-related variation is unlikely to obscure ecologically meaningful spatial differences in B:Ca.

Our findings are also consistent with previous experimental studies in fish that found no detectable effect of short-term pH variation on otolith elemental incorporation (e.g., Hurst et al. 2012; Martino et al. 2017; Cavole et al. 2023). In contrast, studies on invertebrates that precipitate $CaCO_3$ in direct contact with seawater have shown strong pH effects on boron incorporation. In these organisms, reduced pH increases the availability of the borate ion $B(OH)_4^-$, which are more readily incorporated into the carbonate matrix (Levin & Frieder 2015; Norrie et al. 2018; Gagnon et al. 2021). Fish otoliths, however, are internally formed structures. Ions must cross epithelial barriers in the gill or gut and move through the bloodstream to reach the endolymph, where biomineralization occurs (Thomas et al. 2017, Hüssy et al. 2021). This physiological separation from ambient seawater, combined with ion–protein interactions and active homeostatic regulation, likely limits the impact of environmental pH on otolith boron levels (Sturrock et al. 2015; Thomas et al. 2017; Hüssy et al. 2021). Thus, unlike invertebrate structures, fish otoliths may not reliably record ambient pH variation.

While boron may not serve as a sensitive proxy for pH in otoliths, it could still contribute to multi-metric approaches aimed at reconstructing environmental histories. For example, when combined with other elemental or isotopic markers, boron has the potential to strengthen overall interpretations. Integrating multiple proxies may help disentangle the complex interplay of environmental stressors, particularly in systems experiencing simultaneous changes.

**Caveats and future directions**

Our analyses allowed us to examine how individual variation in otolith chemistry arises when fish are held under identical environmental conditions. While temperature differences

between tanks were relatively small (<3 °C), these differences fall within the range that might be encountered between estuaries at regional spatial scales. This is particularly relevant for estuarine or coastal field applications, where small environmental gradients may influence classification accuracy. Expanding the range of temperature conditions in future experiments would allow for clearer assessment of how environmental variation interacts with individual physiology to shape otolith composition. Additionally, although in the experiment we controlled or tracked temperature, dissolved oxygen, pH, and elemental ratios in each tank, as each environmental treatment was represented by a single tank, we cannot rule out tank-specific effects resulting from another unobserved factor.

Ontogenetic influences on otolith chemistry have been documented in numerous in situ studies, where developmental stage, age, or growth-related changes can alter elemental incorporation independently of environmental conditions (Chittaro et al. 2006; Grammer et al. 2017; Reis-Santos et al. 2018; Macdonald et al. 2010). Such effects were unlikely to contribute to the patterns observed here. All individuals were at similar life stages, fish did not differ in size or growth between tanks, and no differences in size or elemental composition were detected between gonadal and non-gonadal fish. These results indicate that ontogeny did not vary systematically across treatments and was therefore not likely a major source of variation in this experiment.

A multi-elemental approach is generally used to reconstruct habitat movements or assign individuals to specific locations (Shima & Swearer 2016; Rogers et al. 2019; Teichert et al. 2024), as multiple environmental variables jointly influence otolith composition (Williams et al. 2018; Reis-Santos et al. 2018). While our study focused on understanding size and temperature effects on individual elements, our findings highlight the value of integrating otolith chemistry with other proxies to reconstruct exposure histories more comprehensively. For example, strontium concentrations may help reconstruct salinity after controlling for size effects, while pH and temperature exposure may be better inferred using isotopic approaches (Høie et al. 2003; Gagnon et al. 2021).

The observed stability of otolith elemental chemistry under different pH conditions also supports its use in multi-metric approaches for reconstructing long-term exposure histories. This is critical, as marine organisms are increasingly exposed to multiple stressors that may interact in

complex and biologically meaningful ways. Future work that connects otolith-based exposure records with measures of individual performance will sharpen predictions of climate change impacts on marine populations and ecosystems (Levin & Frieder 2015, Limburg et al. 2023, Reis-Santos et al. 2023).

## Conclusions

Overall, this work provides additional evidence that otolith trace elemental chemistry is impacted by both environmental and biological factors and that it is unlikely to be impacted by the pH. Our results highlight the need to explicitly consider individual body size when interpreting the results of otolith microchemistry studies in an ecological context. The stability of otolith microchemistry across pH treatments suggests that this technique remains valuable for reconstructing individual environmental exposure, especially when integrated with other calcium carbonate-based approaches to assess responses to multiple interacting stressors.

## ACKNOWLEDGEMENTS

The authors would like to thank Thomas Murphy for assistance with animal husbandry and in the field, Anna Bolm for field assistance, Chris Magel for assistance with setup of the $CO_2$ regulation system, and Jessica Andrade for assistance with laboratory processing of animals. This research was supported by funding from Oregon Sea Grant (R/ECO-48-PD) to JAM and CN and NOAA Ocean Acidification Program funding (award 20903) to TPH**.** CN was also supported by Bonneville Power Administration (Project 1998-014-00). We also thank two anonymous reviewers whose comments greatly improved this manuscript.

## DECLARATIONS

### Funding

This research was supported by Oregon Sea Grant (R/ECO-48-PD) awarded to Jessica A. Miller and Craig R. Norrie, and by NOAA Ocean Acidification Program funding (award 20903) awarded to Thomas P. Hurst. Craig R. Norrie was also supported by Bonneville Power Administration (Project 1998-014-00).

### Conflicts of interest/competing interests

The authors have no relevant financial or non-financial interests to disclose.

## Ethics approval (Sampling permissions, Animal welfare)

The use of animals in this study was carried out in accordance with all applicable institutional and national guidelines at the time that the study was conducted; all work followed American Fisheries Society policies on the Guidelines for Use of Fishes in Research (https://fisheries.org/ docs/policy_useoffishes.pdf) and AVMA (American Veterinary Medical Association) Guidelines on Euthanasia (https://olaw.nih. gov/sites/default/files/Euthanasia2007.pdf). Fish collections and use took place under OSU Institutional Animal Care and Use Committee (IACUC) protocols (IACUC-2020-0129).

## Data and Code availability

Data and code supporting the findings of this study are available from the corresponding author, Craig Norrie, upon reasonable request.

## Authors' contribution statements

Craig Norrie, Thomas Hurst, and Jessica Miller all contributed to the conception and design of the study and to the acquisition of funding. Craig Norrie led data analysis and statistical modelling and drafted the manuscript. Craig Norrie, Thomas Hurst, and Jessica Miller contributed to data interpretation, manuscript revision, and critical evaluation of the work.

## REFERENCES


Amekawa S, Kubota K, Miyairi Y, Seki A, Kawakubo Y, Sakai S, Ajithprasad P, Maemoku H, Osada T, Yokoyama Y (2016) Fossil otoliths, from the Gulf of Kutch, Western India, as a paleo-archive for the mid- to late-Holocene environment. Quaternary International 397:281–288.

Aschenbrenner A, Ferreira BP, Rooker JR (2016) Spatial and temporal variability in the otolith chemistry of the Brazilian snapper *Lutjanus alexandrei* from estuarine and coastal environments. Journal of Fish Biology 89:753–769.

Austin CS, Bond MH, Smith JM, Lowery ED, Quinn TP (2019) Otolith microchemistry reveals partial migration and life history variation in a facultatively anadromous, iteroparous salmonid, bull trout (*Salvelinus confluentus*). Environ Biol Fish 102:95–104.

568 Avigliano E, Pisonero J, Bouchez J, Pouilly M, Domanico A, Sánchez S, Clavijo C, Scarabotti P,
569 Facetti JF, Caffetti JD, del Rosso FR, Llamazares Vegh S, Volpedo AV (2021) Otolith
570 Sr/Ca ratio complements Sr isotopes to reveal fish migration in large basins with
571 heterogeneous geochemical landscapes. Environ Biol Fish 104:277–292.
572 Barnes TC, Gillanders BM (2013) Combined effects of extrinsic and intrinsic factors on otolith
573 chemistry: implications for environmental reconstructions. Can J Fish Aquat Sci
574 70:1159–1166.
575 Beer NA, Wing SR, Hu E (2011) Physical versus biological control of elemental signatures in the
576 otoliths of a temperate reef fish. Marine Ecology Progress Series 433:223–234.
577 Dickson AG, Millero FJ (1987) A comparison of the equilibrium constants for the dissociation of
578 carbonic acid in seawater media. Deep Sea Research Part A. Oceanographic Research
579 Papers 34:1733–1743
580 D'Olivo JP, Sinclair DJ, Rankenburg K, McCulloch MT (2018) A universal multi-trace element
581 calibration for reconstructing sea surface temperatures from long-lived Porites corals:
582 Removing 'vital-effects.' Geochimica et Cosmochimica Acta 239:109–135.
583 Cavole LM, Limburg KE, Gallo ND, Vea Salvanes AG, Ramírez-Valdez A, Levin LA, Oropeza
584 OA, Hertwig A, Liu M-C, McKeegan KD (2023) Otoliths of marine fishes record
585 evidence of low oxygen, temperature and pH conditions of deep Oxygen Minimum
586 Zones. Deep Sea Research Part I: Oceanographic Research Papers 191:103941.
587 Chittaro PM, Gagnon P, Fryer BJ (2006) In situ experiment of ontogenetic variability in the
588 otolith chemistry of Stegastes partitus. Marine Biology 149:1227–1235.
589 Doubleday ZA, Harris HH, Izzo C, Gillanders BM (2014) Strontium Randomly Substituting for
590 Calcium in Fish Otolith Aragonite. Anal Chem 86:865–869. Elsdon TS, Gillanders BM
591 (2005) Alternative life-history patterns of estuarine fish: barium in otoliths elucidates
592 freshwater residency. Can J Fish Aquat Sci 62:1143–1152.
593 Elsdon TS, Gillanders BM (2004) Fish otolith chemistry influenced by exposure to multiple
594 environmental variables. Journal of Experimental Marine Biology and Ecology 313:269–
595 284.
596 Elsdon TS, Gillanders BM (2002) Interactive effects of temperature and salinity on otolith
597 chemistry: challenges for determining environmental histories of fish. Can J Fish Aquat
598 Sci 59:1796–1808.

599 Elsdon TS, Gillanders BM (2003) Relationship between water and otolith elemental
600 concentrations in juvenile black bream *Acanthopagrus butcheri.* Marine Ecology
601 Progress Series 260:263–272.
602 Feely, R. A., Okazaki, R. R., Cai, W.-J., Bednaršek, N., Alin, S. R., Byrne, R. H., & Fassbender,
603 A. (2018). The combined effects of acidification and hypoxia on pH and aragonite
604 saturation in the coastal waters of the California Current ecosystem and the northern Gulf
605 of Mexico. Continental Shelf Research, 152, 50–60.
606 https://doi.org/10.1016/j.csr.2017.11.002
607 Gagnon AC, Gothmann AM, Branson O, Rae JWB, Stewart JA (2021) Controls on boron
608 isotopes in a cold-water coral and the cost of resilience to ocean acidification. Earth and
609 Planetary Science Letters 554:116662.
610 Gattuso JP, Magnan A, Billé R, Cheung WWL, Howes EL, Joos F, Allemand D, Bopp L, Cooley
611 SR, Eakin CM, Hoegh-Guldberg O, Kelly RP, Pörtner H-O, Rogers AD, Baxter JM,
612 Laffoley D, Osborn D, Rankovic A, Rochette J, Sumaila UR, Treyer S, Turley C (2015)
613 Contrasting futures for ocean and society from different anthropogenic CO2 emissions
614 scenarios. Science 349:aac4722.
615 Gillikin DP, Dehairs F, Lorrain A, Steenmans D, Baeyens W, André L (2006) Barium uptake into
616 the shells of the common mussel (*Mytilus edulis*) and the potential for estuarine paleo-
617 chemistry reconstruction. Geochimica et Cosmochimica Acta 70:395–407.
618 Grammer GL, Morrongiello JR, Izzo C, Hawthorne PJ, Middleton JF, Gillanders BM (2017)
619 Coupling biogeochemical tracers with fish growth reveals physiological and
620 environmental controls on otolith chemistry. Ecological Monographs 87:487–507.
621 Høie H, Folkvord A, Otterlei E (2003) Effect of somatic and otolith growth rate on stable
622 isotopic composition of early juvenile cod (*Gadus morhua*) otoliths. Journal of
623 Experimental Marine Biology and Ecology 289:41–58.
624 Hurst TP, Copeman LA, Haines SA, Meredith SD, Daniels K, Hubbard KM (2019) Elevated $CO_2$
625 alters behavior, growth, and lipid composition of Pacific cod larvae. Marine
626 Environmental Research 145:52–65.
627 Hurst TP, Fernandez ER, Mathis JT, Miller JA, Stinson CM, Ahgeak, Ernestine F. (2012)
628 Resiliency of juvenile walleye pollock to projected levels of ocean acidification. Aquatic
629 Biology 17:247–259.

Hüssy K, Haase S, Mion M, Hilvarsson A, Radtke K, Thomsen TB, Krüger-Johnsen M, Casini M, Sturrock AM (2024) Into the wild: coupling otolith and archival tag records to test assumptions underpinning otolith chemistry applications in wild fish. Front Mar Sci 11.

Hüssy K, Limburg KE, de Pontual H, Thomas ORB, Cook PK, Heimbrand Y, Blass M, Sturrock AM (2021) Trace Element Patterns in Otoliths: The Role of Biomineralization. Reviews in Fisheries Science & Aquaculture 29:445–477.

Hüssy K, Gröger J, Heidemann F, Hinrichsen HH, Marohn L (2015) Slave to the rhythm: seasonal signals in otolith microchemistry reveal age of eastern Baltic cod (*Gadus morhua*). ICES J Mar Sci:fsv247. https://doi.org/10.1093/icesjms/fsv247

Izzo C, Doubleday ZA, Grammer GL, Disspain MCF, Ye Q, Gillanders BM (2017) Seasonally resolved environmental reconstructions using fish otoliths. Can J Fish Aquat Sci 74:23–31.

Izzo C, Reis-Santos P, Gillanders BM (2018) Otolith chemistry does not just reflect environmental conditions: A meta-analytic evaluation. Fish and Fisheries 19:441–454.

Izzo C, Doubleday ZA, Schultz AG, Woodcock SH, Gillanders BM (2015) Contribution of water chemistry and fish condition to otolith chemistry: comparisons across salinity environments. Journal of Fish Biology 86:1680–1698.

Jewett L, Romanou A (2017) Ocean Acidification and Other Ocean Changes. Climate Science Special Report: In: *Climate Science Special Report*. Wuebbles DJ, Fahey DW, Hibbard KA, Dokken DJ, Stewart BC, Maycock TK (eds) U.S. Global Change Research Program, Washington, DC, USA, p 364–392

Laetz CA, Zarada K, Lundin JI, Kern J, Sol S, Veggerby K, Chittaro P, Gates J, Hayes KRR, Arthur C, Steinhoff M, Baker M (2024) Growth of Pacific staghorn sculpin (*Leptocottus armatus*) is reduced at contaminated sites in the Lower Duwamish River, Washington. Science of The Total Environment 908:168365.

Lenth RV, Bolker B, Buerkner P, Giné-Vázquez I, emmeans: Estimated Marginal Means, aka Least-Squares Means. R package version 1.11.2-8, https://rvlenth.github.io/emmeans/.

Kraus RT, Secor DH (2004) Incorporation of strontium into otoliths of an estuarine fish. Journal of Experimental Marine Biology and Ecology 302:85–106.

Levin L, Frieder CA (2015) Geochemical Proxies for Estimating Faunal Exposure to Ocean Acidification. Oceanography 28:68–73.

661 Limburg KE, Casini M (2018) Effect of Marine Hypoxia on Baltic Sea Cod Gadus morhua:
662 Evidence From Otolith Chemical Proxies. Frontiers in Marine Science 5.
663 Limburg KE, Heimbrand Y, Kuliński K (2023) Marked recent declines in boron in Baltic Sea cod
664 otoliths – a bellwether of incipient acidification in a vast hypoxic system? Biogeosciences
665 20:4751–4760.
666 Limburg KE, Walther BD, Lu Z, Jackman G, Mohan J, Walther Y, Nissling A, Weber PK,
667 Schmitt AK (2015) In search of the dead zone: Use of otoliths for tracking fish exposure
668 to hypoxia. Journal of Marine Systems 141:167–178.
669 Loewen TN, Carriere B, Reist JD, Halden NM, Anderson WG (2016) Linking physiology and
670 biomineralization processes to ecological inferences on the life history of fishes.
671 Comparative Biochemistry and Physiology Part A: Molecular & Integrative Physiology
672 202:123–140.
673 Martino J, Doubleday ZA, Woodcock SH, Gillanders BM (2017) Elevated carbon dioxide and
674 temperature affects otolith development, but not chemistry, in a diadromous fish. Journal
675 of Experimental Marine Biology and Ecology 495:57–64.
676 Matta ME, Miller JA, Short JA, Helser TE, Hurst TP, Rand KM, Ormseth OA (2019) Spatial and
677 temporal variation in otolith elemental signatures of age-0 Pacific cod (*Gadus*
678 *macrocephalus*) in the Gulf of Alaska. Deep Sea Research Part II: Topical Studies in
679 Oceanography 165:268–279.
680 Mateo I, Durbin EG, Bengtson DA, Kingsley R, Swart PK, Durant D (2012) Spatial and
681 Temporal Variation in Otolith Chemistry for Tautog (Tautoga onitis) along the US
682 Northeast Coast. NENA 19:201–216.
683 Macdonald JI, Crook DA (2010) Variability in Sr:Ca and Ba:Ca ratios in water and fish otoliths
684 across an estuarine salinity gradient. Marine Ecology Progress Series 413:147–161
685 Miller JA (2011) Effects of water temperature and barium concentration on otolith composition
686 along a salinity gradient: Implications for migratory reconstructions. Journal of
687 Experimental Marine Biology and Ecology 405:42–52.
688 Miller JA. (2009) The effects of temperature and water concentration on the otolith incorporation
689 of barium and manganese in black rockfish *Sebastes melanops*. Journal of Fish Biology
690 75:39–60.

691 Miller JA (2007) Scales of variation in otolith elemental chemistry of juvenile staghorn sculpin
692 (*Leptocottus armatus*) in three Pacific Northwest estuaries. Mar Biol 151:483–494.
693 Miller JA, Gray A, Merz J (2010) Quantifying the contribution of juvenile migratory phenotypes
694 in a population of Chinook salmon *Oncorhynchus tshawytscha*. Marine Ecology Progress
695 Series 408:227–240.
696 Miller JA, Hurst TP (2020) Growth Rate, Ration, and Temperature Effects on Otolith Elemental
697 Incorporation. Frontiers in Marine Science 7.
698 Mohan JA, Walther BD (2015) Spatiotemporal Variation of Trace Elements and Stable Isotopes
699 in Subtropical Estuaries: II. Regional, Local, and Seasonal Salinity-Element
700 Relationships. Estuaries and Coasts 38:769–781.
701 Norrie C, Dunphy B, Roughan M, Weppe S, Lundquist C (2020) Spill-over from aquaculture
702 may provide a larval subsidy for the restoration of mussel reefs. Aquaculture
703 Environment Interactions 12:231–249.
704 Norrie C, Morgan C, Burke B, Weitkamp L, Miller J (2022) Freshwater growth can provide a
705 survival advantage to Interior Columbia River spring Chinook salmon after ocean entry.
706 Mar Ecol Prog Ser 691:131–149.
707 Norrie CR, Dunphy BJ, Ragg NLC, Lundquist CJ (2019) Comparative influence of genetics,
708 ontogeny and the environment on elemental fingerprints in the shell of *Perna*
709 *canaliculus*. Sci Rep 9:8533.
710 Norrie CR, Dunphy BJ, Ragg NLC, Lundquist CJ (2018) Ocean acidification can interact with
711 ontogeny to determine the trace element composition of bivalve shell. Limnology and
712 Oceanography Letters 3:393–400.
713 Pease AA, Jacobs GR, Mendoza-Carranza M, Rodiles-Hernández R, Wenger SJ, Capps KA
714 (2023) Otolith microchemistry highlights the importance of extensive connectivity for
715 conservation of an iconic migratory fish in a large tropical river basin. Aquatic
716 Conservation: Marine and Freshwater Ecosystems 2023:1–12.
717 Reis-Santos P, Tanner SE, Elsdon TS, Cabral HN, Gillanders BM (2013) Effects of temperature,
718 salinity and water composition on otolith elemental incorporation of *Dicentrarchus*
719 *labrax*. Journal of Experimental Marine Biology and Ecology 446:245–252.

720 Reis-Santos P, Vasconcelos RP, Tanner SE, Fonseca VF, Cabral HN, Gillanders BM (2018)
721 Extrinsic and intrinsic factors shape the ability of using otolith chemistry to characterize
722 estuarine environmental histories. Marine Environmental Research 140:332–341.
723 Reis-Santos P, Gillanders BM, Sturrock AM, Izzo C, Oxman DS, Lueders-Dumont JA, Hüssy K,
724 Tanner SE, Rogers T, Doubleday ZA, Andrews AH, Trueman C, Brophy D, Thiem JD,
725 Baumgartner LJ, Willmes M, Chung M-T, Charapata P, Johnson RC, Trumble S,
726 Heimbrand Y, Limburg KE, Walther BD (2023) Reading the biomineralized book of life:
727 expanding otolith biogeochemical research and applications for fisheries and ecosystem-
728 based management. Rev Fish Biol Fisheries 33:411–449.
729 Rogers TA, Fowler AJ, Steer MA, Gillanders BM (2019) Discriminating Natal Source
730 Populations of a Temperate Marine Fish Using Larval Otolith Chemistry. Frontiers in
731 Marine Science 6.
732 Shima JS, Swearer SE (2016) Evidence and population consequences of shared larval dispersal
733 histories in a marine fish. Ecology 97:25–31.
734 Stanley RRE, Bradbury IR, DiBacco C, Snelgrove PVR, Thorrold SR, Killen SS (2015)
735 Environmentally mediated trends in otolith composition of juvenile Atlantic cod (*Gadus*
736 *morhua*). ICES Journal of Marine Science 72:2350–2363.
737 Sturrock AM, Hunter E, Milton JA, Eimf, Johnson RC, Waring CP, Trueman CN (2015)
738 Quantifying physiological influences on otolith microchemistry. Methods in Ecology and
739 Evolution 6:806–816.
740 Tanaka K, Holcomb M, Takahashi A, Kurihara H, Asami R, Shinjo R, Sowa K, Rankenburg K,
741 Watanabe T, McCulloch M (2015) Response of *Acropora digitifera* to ocean
742 acidification: constraints from δ11B, Sr, Mg, and Ba compositions of aragonitic skeletons
743 cultured under variable seawater pH. Coral Reefs 34:1139–1149.
744 Tanner SE, Reis-Santos P, Cabral HN (2016) Otolith chemistry in stock delineation: A brief
745 overview, current challenges and future prospects. Fisheries Research 173:206–213.
746 Teichert N, Tabouret H, Lizé A, Daverat F, Acou A, Trancart T, Virag L-S, Pécheyran C,
747 Feunteun E, Carpentier A (2024) Quantifying larval dispersal portfolio in seabass
748 nurseries using otolith chemical signatures. Marine Environmental Research 196:106426.
749 Thébault J, Chauvaud L, L'Helguen S, Clavier J, Barats A, Jacquet Sé, PÉcheyran C, Amouroux
750 D (2009) Barium and molybdenum records in bivalve shells: Geochemical proxies for

751 phytoplankton dynamics in coastal environments? Limnology and Oceanography
752 54:1002–1014.
753 Thomas ORB, Ganio K, Roberts BR, Swearer SE (2017) Trace element–protein interactions in
754 endolymph from the inner ear of fish: implications for environmental reconstructions
755 using fish otolith chemistry†. Metallomics 9:239–249.
756 Tian H, Liu J, Cao L, Dou S (2021) Temperature and salinity effects on strontium and barium
757 incorporation into otoliths of flounder *Paralichthys olivaceus* at early life stages.
758 Fisheries Research 239:105942.
759 Walther BD, Thorrold SR (2006) Water, not food, contributes the majority of strontium and
760 barium deposited in the otoliths of a marine fish. Marine Ecology Progress Series
761 311:125–130.
762 Wanamaker Jr AD, Kreutz KJ, Wilson T, Borns Jr HW, Introne DS, Feindel S (2008)
763 Experimentally determined Mg/Ca and Sr/Ca ratios in juvenile bivalve calcite for Mytilus
764 edulis: implications for paleotemperature reconstructions. Geo-Mar Lett 28:359–368.
765 Webb SD, Woodcock SH, Gillanders BM (2012) Sources of otolith barium and strontium in
766 estuarine fish and the influence of salinity and temperature. Marine Ecology Progress
767 Series 453:189–199.
768 Williams J, Jenkins GP, Hindell JS, Swearer SE (2018) Fine-scale variability in elemental
769 composition of estuarine water and otoliths: Developing environmental markers for
770 determining larval fish dispersal histories within estuaries. Limnology and Oceanography
771 63:262–277.
772 Wu, W., Lundquist, C. J., & Jeffs, A. G. (2025). Spatial resolution of shell microchemistry for
773 tracking dispersing pelagic mussels in a large open embayment in northern New Zealand.
774 Marine and Freshwater Research, 76, MF24065.
775 Wuebbles DJ, Fahey DW, Hibbard KA, Dokken DJ, Stewart BC, Maycock TK (2017) Climate
776 Science Special Report: Fourth National Climate Assessment, Volume I. U.S. Global
777 Change Research Program.
778

**SUPPLEMENTARY MATERIALS**

**Norrie, Hurst, and Miller. supplementary materials: Environmental and Biological Drivers of Otolith Trace Element Composition in Staghorn Sculpin *(Leptocottus armatus*)**

**Journal:** Marine Biology

**Authors:** Craig R. Norrie*[1,2], Thomas P. Hurst, Jessica A. Miller

*Corresponding author: cnorrie@uw.edu

[1]Cooperative Institute for Marine Ecosystem and Resources Studies, Oregon State University, Newport, OR 97365, USA. ORCID: 0000-0003-0085-7314

[2]Current Address: School of Aquatic and Fishery Sciences. University of Washington Seattle, Washington, USA.

**Manuscript title:** Environmental and Biological Drivers of Otolith Trace Element Composition in Staghorn Sculpin (*Leptocottus armatus*)

***Supplementary Tables***

Table S1. Mean otolith increment widths (± SEM) of fish from each tank

| Temperature | pH | Increment Width |
|---|---|---|
| 11.5 | Ambient | 0.64 (± 0.23) |
| | Medium | 0.93 (± 0.26) |
| | Low | 0.95 (± 0.17) |
| 14 | Ambient | 0.86 (± 0.27) |
| | Medium | 1.19 (± 0.22) |
| | Low | 0.59 (± 0.23) |

793

Table S2. Results of linear models examining covariates of final length, final mass, length specific and mass specific growth rates (LSGR and MSGR), and length–weight residuals (LWR) for Mn:Ca, Co:Ca, and Mg:Ca.

| TE:Ca | Covariate | Temp x pH x covariate | pH x covariate | Temp x covariate | Temp pH | Covariate | pH | Temp | Model adjusted $R^2$ |
|---|---|---|---|---|---|---|---|---|---|
| Mn:Ca | Final Length | $F_{2,42} = 1.06$, $p = 0.36$ | $F_{2,42} = 0.08$, $p = 0.93$ | $F_{1,42} = 3.49$, $p = 0.07$ | $F_{2,42} = 0.21$, $p = 0.81$ | $F_{1,42} = 5.53$, $p = 0.02$ | $F_{2,42} = 0.38$, $p = 0.69$ | $F_{1,42} = 2.04$, $p = 0.16$ | 0.062 |
| | Final Mass | $F_{2,41} = 0.97$, $p = 0.38$ | $F_{2,41} = 0.62$, $p = 0.55$ | $F_{1,41} = 3.12$, $p = 0.07$ | $F_{2,41} = 0.36$, $p = 0.75$ | $F_{1,41} = 5.32$, $p = 0.03$ | $F_{2,41} = 0.07$, $p = 0.93$ | $F_{1,41} = 1.98$, $p = 0.15$ | 0.036 |
| | LSGR | $F_{2,42} = 3.39$, $p = 0.04$ | $F_{2,42} = 6.25$, $p = 0.004$ | $F_{1,42} = 0.42$, $p = 0.52$ | $F_{2,42} = 1.78$, $p = 0.18$ | $F_{1,42} = 5.47$, $p = 0.02$ | $F_{2,42} = 6.18$, $p = 0.006$ | $F_{1,42} = 1.05$, $p = 0.31$ | -0.018 |
| | MSGR | $F_{2,41} = 0.81$, $p = 0.45$ | $F_{2,41} = 0.40$, $p = 0.68$ | $F_{1,41} = 1.25$, $p = 0.27$ | $F_{2,41} = 1.00$, $p = 0.38$ | $F_{1,41} = 0.86$, $p = 0.36$ | $F_{2,41} = 0.01$, $p = 0.99$ | $F_{1,41} = 0.82$, $p = 0.37$ | -0.075 |
| | LWR | $F_{2,42} = 0.35$, $p = 0.71$ | $F_{2,42} = 2.00$, $p = 0.15$ | $F_{1,42} = 0.07$, $p = 0.79$ | $F_{2,42} = 0.13$, $p = 0.87$ | $F_{1,42} = 0.02$, $p = 0.88$ | $F_{2,42} = 0.02$, $p = 0.98$ | $F_{1,42} = 0.48$, $p = 0.49$ | -0.11 |
| Co:Ca | Final Length | $F_{2,42} = 3.78$, $p = 0.03$ | $F_{2,42} = 0.01$, $p = 0.97$ | $F_{1,42} = 5.35$, $p = 0.03$ | $F_{2,42} = 0.63$, $p = 0.54$ | $F_{1,42} = 2.42$, $p = 0.13$ | $F_{2,42} = 0.20$, $p = 0.83$ | $F_{1,42} = 0.09$, $p = 0.76$ | 0.100 |
| | Final Mass | $F_{2,41} = 1.61$, $p = 0.21$ | $F_{2,41} = 0.13$, $p = 0.93$ | $F_{1,41} = 2.02$, $p = 0.15$ | $F_{2,41} = 0.78$, $p = 0.46$ | $F_{1,41} = 0.82$, $p = 0.37$ | $F_{2,41} = 0.04$, $p = 0.96$ | $F_{1,41} = 0.29$, $p = 0.59$ | -0.023 |
| | MSGR | $F_{2,41} = 2.20$, $p = 0.12$ | $F_{2,41} = 1.13$, $p = 0.33$ | $F_{1,41} = 0.56$, $p = 0.46$ | $F_{2,41} = 0.78$, $p = 0.46$ | $F_{1,41} = 2.03$, $p = 0.16$ | $F_{2,41} = 0.61$, $p = 0.56$ | $F_{1,41} = 0.30$, $p = 0.79$ | -0.074 |
| | LSGR | $F_{2,42} = 2.20$, $p = 0.12$ | $F_{2,42} = 1.13$, $p = 0.33$ | $F_{1,42} = 0.56$, $p = 0.46$ | $F_{2,42} = 0.78$, $p = 0.46$ | $F_{1,42} = 2.03$, $p = 0.16$ | $F_{2,42} = 0.61$, $p = 0.56$ | $F_{1,42} = 0.30$, $p = 0.79$ | 0.019 |
| | LWR | $F_{2,42} = 1.61$, $p = 0.21$ | $F_{2,42} = 0.58$, $p = 0.56$ | $F_{1,42} = 0.01$, $p = 0.93$ | $F_{2,42} = 0.79$, $p = 0.46$ | $F_{1,42} = 0.61$, $p = 0.54$ | $F_{2,42} = 0.02$, $p = 0.88$ | $F_{1,42} = 0.33$, $p = 0.57$ | -0.082 |
| Mg:Ca | Final Length | $F_{2,42} = 4.75$, $p = 0.01$ | $F_{2,42} = 1.15$, $p = 0.32$ | $F_{1,42} = 3.54$, $p = 0.07$ | $F_{2,42} = 0.94$, $p = 0.40$ | $F_{1,42} = 1.70$, $p = 0.20$ | $F_{2,42} = 0.19$, $p = 0.83$ | $F_{1,42} = 0.15$, $p = 0.70$ | 0.138 |
| | Final Mass | $F_{2,41} = 2.56$, $p = 0.06$ | $F_{2,41} = 0.82$, $p = 0.45$ | $F_{1,41} = 1.17$, $p = 0.22$ | $F_{2,41} = 1.28$, $p = 0.29$ | $F_{1,41} = 1.43$, $p = 0.24$ | $F_{2,41} = 0.11$, $p = 0.90$ | $F_{1,41} = 0.09$, $p = 0.76$ | 0.049 |
| | MSGR | $F_{2,41} = 0.42$, $p = 0.66$ | $F_{2,41} = 1.17$, $p = 0.32$ | $F_{1,41} = 0.10$, $p = 0.75$ | $F_{2,41} = 1.97$, $p = 0.15$ | $F_{1,41} = 1.42$, $p = 0.24$ | $F_{2,41} = 0.38$, $p = 0.93$ | $F_{1,41} = 0.00$, $p = 0.99$ | -0.043 |

| | | | | | | | | | |
|---|---|---|---|---|---|---|---|---|---|
| | LSGR | $F_{2,42} = 0.04$, $p = 0.96$ | $F_{2,42} = 1.14$, $p = 0.33$ | $F_{1,42} = 2.31$, $p = 0.14$ | $F_{2,42} = 0.20$, $p = 0.82$ | $F_{1,42} = 2.35$, $p = 0.13$ | $F_{2,42} = 0.62$, $p = 0.65$ | $F_{1,42} = 0.12$, $p = 0.73$ | -0.049 |
| | LWR | $F_{2,42} = 1.64$, $p = 0.21$ | $F_{2,42} = 0.84$, $p = 0.44$ | $F_{1,42} = 0.11$, $p = 0.75$ | $F_{2,42} = 1.33$, $p = 0.28$ | $F_{1,42} = 0.20$, $p = 0.82$ | $F_{2,42} = 0.02$, $p = 0.98$ | $F_{1,42} = 0.02$, $p = 0.90$ | -0.063 |

795

796

797

Table S3. Results of the linear models examining covariates of final length, final mass, length specific and mass specific (MSGR) growth rates, and length weight residuals (LWR) for each trace element calcium ratio (TE:Ca) investigated in this work.

| TE:Ca | Covariate | Temp x pH x covariate | pH x covariate | Temp x covariate | Temp pH | Covariate | pH | Temp | Model adjusted $R^2$ |
|---|---|---|---|---|---|---|---|---|---|
| Sr:Ca | Final Length | $F_{2,42} = 0.07$, p = 0.93 | $F_{2,42} = 0.98$, p = 0.39 | $F_{1,42} = 5.64$, p = 0.02 | $F_{2,42} = 2.18$, p = 0.13 | $F_{1,42} = 22.84$, p = 0.00 | $F_{2,42} = 0.38$, p = 0.69 | $F_{1,42} = 5.52$, p = 0.02 | 0.362 |
| | Final Mass | $F_{2,41} = 0.17$, p = 0.84 | $F_{2,41} = 0.53$, p = 0.59 | $F_{1,41} = 5.77$, p = 0.02 | $F_{2,41} = 2.75$, p = 0.08 | $F_{1,41} = 18.45$, p = 0.00 | $F_{2,41} = 0.38$, p = 0.69 | $F_{1,41} = 4.79$, p = 0.03 | 0.330 |
| | LSGR | $F_{2,42} = 0.33$, p = 0.72 | $F_{2,42} = 0.73$, p = 0.49 | $F_{1,42} = 0.34$, p = 0.56 | $F_{2,42} = 1.31$, p = 0.28 | $F_{1,42} = 1.63$, p = 0.21 | $F_{2,42} = 0.24$, p = 0.79 | $F_{1,42} = 3.49$, p = 0.07 | -0.006 |
| | MSGR | $F_{2,41} = 1.00$, p = 0.38 | $F_{2,41} = 1.81$, p = 0.18 | $F_{1,41} = 0.88$, p = 0.35 | $F_{2,41} = 2.15$, p = 0.13 | $F_{1,41} = 1.57$, p = 0.22 | $F_{2,41} = 0.28$, p = 0.76 | $F_{1,41} = 3.54$, p = 0.07 | 0.095 |
| | LWR | $F_{2,42} = 1.45$, p = 0.25 | $F_{2,42} = 1.91$, p = 0.16 | $F_{1,42} = 0.12$, p = 0.73 | $F_{2,42} = 2.28$, p = 0.12 | $F_{1,42} = 0.90$, p = 0.35 | $F_{2,42} = 0.31$, p = 0.73 | $F_{1,42} = 3.51$, p = 0.07 | 0.092 |
| B:Ca | Final Length | $F_{2,42} = 1.52$, p = 0.23 | $F_{2,42} = 0.75$, p = 0.48 | $F_{1,42} = 0.07$, p = 0.79 | $F_{2,42} = 2.31$, p = 0.11 | $F_{1,42} = 7.19$, p = 0.01 | $F_{2,42} = 0.35$, p = 0.71 | $F_{1,42} = 1.60$, p = 0.21 | 0.127 |
| | Final Mass | $F_{2,41} = 2.62$, p = 0.09 | $F_{2,41} = 0.77$, p = 0.47 | $F_{1,41} = 0.04$, p = 0.85 | $F_{2,41} = 3.18$, p = 0.05 | $F_{1,41} = 4.18$, p = 0.05 | $F_{2,41} = 0.87$, p = 0.43 | $F_{1,41} = 1.04$, p = 0.31 | 0.149 |
| | LSGR | $F_{2,42} = 0.02$, p = 0.99 | $F_{2,42} = 0.17$, p = 0.85 | $F_{1,42} = 0.28$, p = 0.60 | $F_{2,42} = 1.46$, p = 0.24 | $F_{1,42} = 2.60$, p = 0.12 | $F_{2,42} = 0.29$, p = 0.75 | $F_{1,42} = 1.32$, p = 0.26 | -0.058 |
| | MSGR | $F_{2,41} = 0.41$, p = 0.67 | $F_{2,41} = 2.38$, p = 0.11 | $F_{1,41} = 0.99$, p = 0.33 | $F_{2,41} = 2.39$, p = 0.10 | $F_{1,41} = 2.40$, p = 0.13 | $F_{2,41} = 0.82$, p = 0.45 | $F_{1,41} = 0.98$, p = 0.33 | 0.093 |

| | | | | | | | | | |
|---|---|---|---|---|---|---|---|---|---|
| | LWR | $F_{2,42} = 0.08$, p = 0.92 | $F_{2,42} = 3.03$, p = 0.06 | $F_{1,42} = 0.17$, p = 0.68 | $F_{2,42} = 2.13$, p = 0.13 | $F_{1,42} = 0.21$, p = 0.65 | $F_{2,42} = 0.53$, p = 0.59 | $F_{1,42} = 4.62$, p = 0.04 | 0.069 |
| Ba:Ca | Final Length | $F_{2,42} = 3.86$, p = 0.03 | $F_{2,42} = 2.14$, p = 0.13 | $F_{1,42} = 0.49$, p = 0.49 | $F_{2,42} = 2.45$, p = 0.10 | $F_{1,42} = 6.22$, p = 0.02 | $F_{2,42} = 0.83$, p = 0.44 | $F_{1,42} = 6.77$, p = 0.01 | 0.284 |
| | Final Mass | $F_{2,41} = 2.69$, p = 0.08 | $F_{2,41} = 1.83$, p = 0.17 | $F_{1,41} = 0.35$, p = 0.56 | $F_{2,41} = 2.71$, p = 0.08 | $F_{1,41} = 5.13$, p = 0.03 | $F_{2,41} = 0.71$, p = 0.50 | $F_{1,41} = 5.54$, p = 0.02 | 0.234 |
| | LSGR | $F_{2,42} = 0.82$, p = 0.45 | $F_{2,42} = 0.59$, p = 0.56 | $F_{1,42} = 0.09$, p = 0.77 | $F_{2,42} = 1.66$, p = 0.20 | $F_{1,42} = 0.72$, p = 0.40 | $F_{2,42} = 0.62$, p = 0.54 | $F_{1,42} = 5.05$, p = 0.03 | 0.040 |
| | MSGR | $F_{2,41} = 0.05$, p = 0.95 | $F_{2,41} = 1.14$, p = 0.33 | $F_{1,41} = 0.44$, p = 0.51 | $F_{2,41} = 1.69$, p = 0.20 | $F_{1,41} = 1.58$, p = 0.22 | $F_{2,41} = 0.57$, p = 0.57 | $F_{1,41} = 4.44$, p = 0.04 | 0.043 |
| | LWR | $F_{2,42} = 2.99$, p = 0.06 | $F_{2,42} = 0.26$, p = 0.78 | $F_{1,42} = 0.01$, p = 0.92 | $F_{2,42} = 2.87$, p = 0.07 | $F_{1,42} = 0.06$, p = 0.81 | $F_{2,42} = 0.79$, p = 0.46 | $F_{1,42} = 1.04$, p = 0.31 | 0.094 |

798

799

***Supplementary figures***

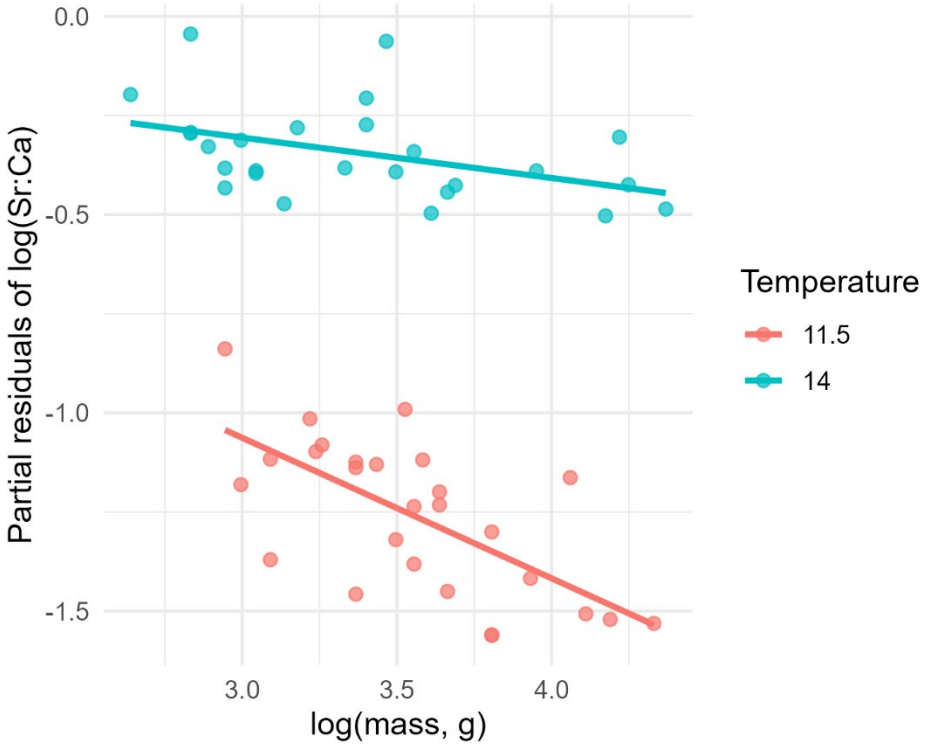


Figure S1. Partial residuals from the linear model relating log(Sr:Ca) to log(mass) and temperature. Points show partial residuals and lines show fitted relationships for each temperature. This plot illustrates the size–temperature structure present in the model.

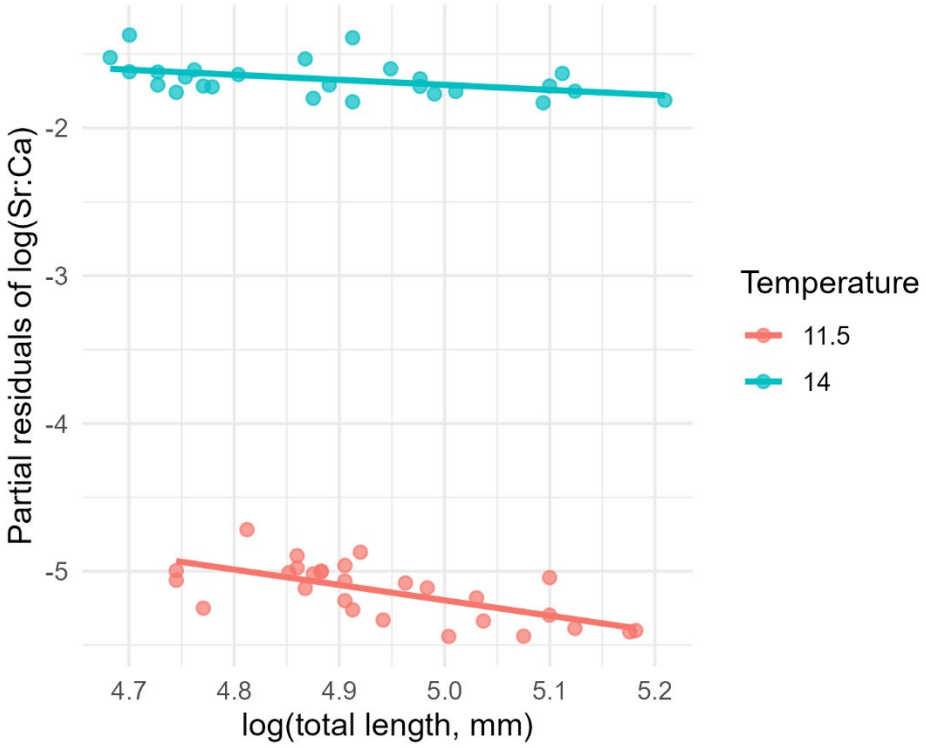


Figure S2. Partial residuals from the linear model relating log(Sr:Ca) to log(total length) and temperature. Points represent partial residuals and lines represent fitted relationships for each temperature. This plot shows the relationship between size and Sr:Ca within each temperature treatment.

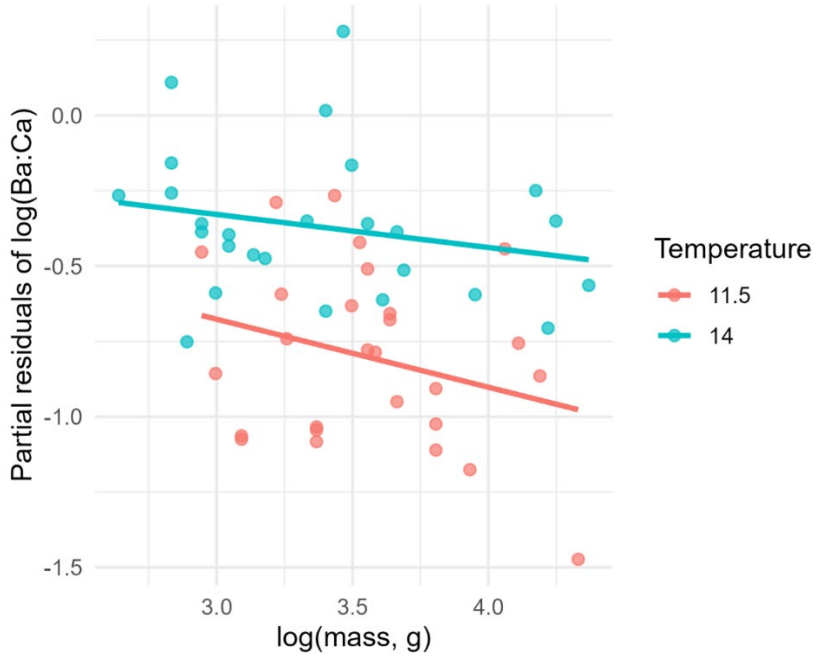


Figure S3. Partial residuals from the linear model relating log(Ba:Ca) to log(mass) and temperature. Points show partial residuals and fitted lines are shown for each temperature. This plot provides the diagnostic view of the mass–Ba:Ca relationship used in the model comparison.

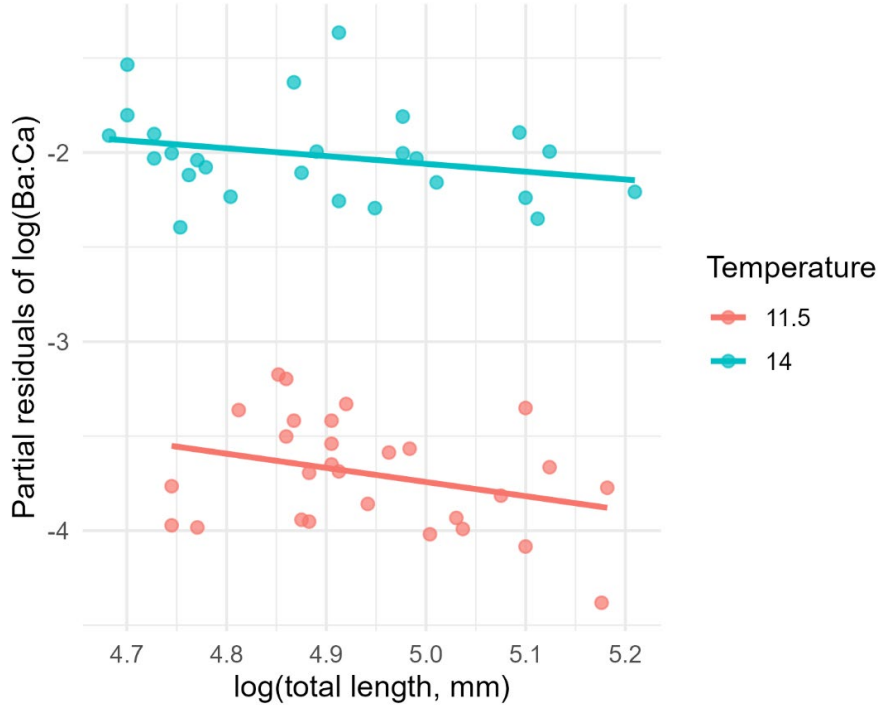


Figure S4. Partial residuals from the linear model relating log(Ba:Ca) to log(total length) and temperature. Points show partial residuals and lines show fitted relationships for each temperature. This plot provides the diagnostic view of the length–Ba:Ca relationship.